PREDICTING THE EFFECTS OF FREEZING AND THAWING ON PAVEMENT SUPPORT

WI/SPR-02-98

FINAL REPORT

July 1998

PB99-162810

TECHNICAL REPORT DOCUMENTATION PAGE

DT1487 97

Wisconsin Department of Transportation

1. Report Number	2. Government Accession Number	3. Recipient's Catalog Number
WI/SPR-02-98		

4. Title and Subtitle	5. Report Date / 6. Performing Organization Code
Predicting the Effects of Freezing and Thawing on Pavement Support	5. Report Date: 10/13/98 6. Performing Organization Code
7. Author(s) Benson, Craig H.; Bosscher, Peter J.; Jong,Da-tong	8. Performing Organization Report Number
9. Performing Organization Name and Address University of Wisconsin - Madison Environmental Geotechnics Program Dept. of Civil and Environmental Engineering 2214 Engineering Hall 1415 Engineering Drive Madison, WI. 53704-2507	10. Work unit Number (TRAIS) 11. Contract or Grant Number
12. Sponsoring Agency Name and Address Wisconsin Dept. of Transportation DTID / Bureau of Highway Construction 3502 Kinsman Blvd. Madison, WI. 53704-2507	13. Type of Report and Period Covered 14. Sponsoring Agency Code

15. Supplementary Notes

16. Abstract

The objective of this study was to develop a method to predict the timing of weight limits on secondary highways in Wisconsin. Two types of weight limits are of interest: overloads when the pavement is frozen and weight restrictions during thawing and post-thawing recovery period. To meet this objective, three sections of secondary highways with flexible pavements were instrumented and monitored fo determine how freezing, thawing, and post-thaw recovery affect pavement stiffness. Data collected from these sites were used to develop a computer model [UWFrost] that can be used to predict seasonal changes in the support capacity of pavements. The computer model is operated from a Microsoft Excel spreadsheet.

Freezing and thawing were found to have a significant effect on the stiffness and capacity of flexible pavements. The pavement stiffens during winter when the base freezes, and softens substantially when the base and subgrade thaw. A gradual recovery process occurs after thawing is complete during which the pavement stiffens. This recovery process extends through a non-dimensional modulus ratio function that varies with time. This function is an intrinsic component of UWFrost.

UW Frost simulates how freezing and thawing affect the stiffness and capacity of pavements. The user enters meteorological data, pavement location, pavement layer geometry, and timing criteria. A one-dimensional heat transfer module uses the input to define the moduli of the pavement layers, which are used in a layered elastic analysis. The elastic analysis is used iteratively to determine the load that induces no more damage than a design load applied during late summer. This load is referred to as the equivalent damage load [EDL]. EDLs are defined for fatigue and rutting damage.

UWFrost computes EDLs for each day during the prediction period selected by the user. EDLs are as much as three times higher than design loads when the base and subgrade are frozen. At the end of thaw, when the pavement reaches its softest condition, the EDL can be less than one-half the design load.

17. Key Words	18. Distribution Statement
Weight limits; Pavement support; Freeze / Thaw	

19. Security Classification (of this report)	20. Security Classification (of this page)	21. No.of Pages	22. Price
		52	

PREDICTING THE EFFECTS OF FREEZING AND THAWING ON PAVEMENT SUPPORT

WI/SPR-02-98

FINAL REPORT

Prof. Craig H. Benson
Dept. of Civil & Environmental Engineering
University of Wisconsin-Madison
1415 Engineering Drive
Madison, WI 53706

Prof. Peter J. Bosscher
Dept. of Civil & Environmental Engineering
University of Wisconsin-Madison
1415 Engineering Drive
Madison, WI 53706

Mr. Da-Tong Jong
Dept. of Civil & Environmental Engineering
University of Wisconsin-Madison
1415 Engineering Drive
Madison, WI 53706

July 1998

For

WISCONSIN DEPT. OF TRANSPORATION
Division of Transportation Infrastructure Development
Bureau of Highway Construction
Pavement Section
3502 Kinsman Blvd., Madison, WI 53704

EXECUTIVE SUMMARY

The objective of this study was to develop a method to predict the timing of weight limits on secondary highways in Wisconsin. Two types of weight limits are of interest: overloads when the pavement is frozen and weight restrictions during thawing and the post-thawing recovery period. To meet this objective, three sections of secondary highways with flexible pavements were instrumented and monitored to determine how freezing, thawing, and post-thaw recovery affect pavement stiffness. Data collected from these sites were used to develop a computer model (UWFrost) that can be used to predict seasonal changes in the capacity of pavements. The computer model is operated from a Microsoft Excel spreadsheet.

Freezing and thawing were found to have a significant effect on the stiffness and capacity of flexible pavements. The pavement stiffens during winter when the base freezes, and softens substantially when the base and subgrade thaw. A gradual recovery process occurs after thawing is complete during which the pavement stiffens. This recovery process extends through mid-summer. These changes in stiffness can be characterized by a non-dimensional modulus ratio function that varies with time. This function is an intrinsic component of UWFrost.

UWFrost simulates how freezing and thawing affect the stiffness and capacity of pavements. The user enters meteorological data, pavement location, pavement layer geometry, and timing criteria. A one-dimensional heat transfer module uses the input to define the frost depth and/or the thaw depth. Historical meteorological data are used to predict subsurface thermal conditions in the future. Predicted thermal conditions in the subsurface are used to define the moduli of the pavement layers, which are used in a layered elastic analysis. The elastic analysis is used iteratively to determine the load that induces no more damage than a design load applied during late summer. This load is referred to as the equivalent damage load (EDL). EDLs are defined for fatigue and rutting damage.

UWFrost computes EDLs for each day during the prediction period selected by the user. EDLs are as much as three times higher than design loads when the base and subgrade are frozen. At the end of thaw, when the pavement reaches its softest condition, the EDL can be less than one-half the design load.

ACKNOWLEDGEMENT

This study was conducted for the Wisconsin Dept. of Transportation (WisDOT) which provided the funds to perform the work and the project oversight and direction, as well as the falling weight deflectometer used in the study. This support is gratefully acknowledged. Many persons from WisDOT made this project possible. These people include Robert Schmeidlin, Terry Rutkowski, Thomas Martinelli, James Voborsky, and other members of the Technical Oversight Committee. Mark Goodhue, Mark Samuelson, Brain Albrecht, and Douglas Detmers, all students from the University of Wisconsin-Madison, also assisted with the study. Dr. Nazli Yesiller of Wayne State University assisted in an early portion of the study. Myron Tanner of Measurement Systems Technology helped install the instrumentation.

Although WisDOT approved this report, the opinions presented in it are solely of the authors.

TABLE OF CONTENTS

SECTION 1
INTRODUCTION

In northern regions, pavements are subjected to freezing in the winter and thawing in the spring. Flexible pavement moduli increase in the winter because the unbound base and subgrade freeze, and because the viscosity of asphalt increases. As a result, the frozen pavement can sustain traffic loads greater than the design loads without being damaged. In contrast, during the spring thaw, the base and subgrade become saturated with water as the soil thaws and the snow melts. Consequently, the moduli of the pavement layers decrease, often below the pre-freezing condition. The weakened pavement cannot support the load it was originally designed for, and thus damage occurs (AASHTO 1993, Ullidtz 1987, US Army 1985, Andersland and Ladanyi 1994, Janoo and Berg 1991). These effects are shown conceptually in Fig. 1.1.

Historically, many kilometers of highway have been built using local base and subbase materials that may be frost-susceptible. Additionally, constructing pavement structures to prevent damage during thaw-weakening is not always possible. Consequently, load restrictions are often applied to prevent pavement damage during the thaw-weakening period (Mahoney et al., 1985; Thomassen and Eirum, 1982). To maximize the benefit of the load restrictions and reach an optimal state between pavement usage and protection, decisions must be carefully made regarding where load restrictions are required, when restrictions are applied, and the maximum load that is specified. Unfortunately, procedures and criteria used for load restrictions during the spring thaw period are often poorly defined, inadequate, and non-uniform (Rwebrangira et al. 1987, Rutherford and Mahoney 1986, Mahoney et al. 1985, 1987; McBane and Hanek 1986, FHWA 1987, Thomassen and Eirum 1982, Janoo and Berg 1990, 1996).

The objective of this project was to develop a rational method to determine the timing of permissible overloads when secondary flexible pavements are frozen and the timing of load restrictions during the spring thaw. To meet this objective, a computer model named UWFROST was developed that predicts loads a pavement can withstand without incurring excessive damage as the stiffness of the subsurface changes due to freezing and thawing. Three sections of secondary highways were instrumented and monitored to collect data needed for developing algorithms employed by the model.

This report describes the field data that were collected and how the data were incorporated into the model UWFrost. The model is described in detail in Bosscher et al. (1998). Section 2 describes the basis for conducting the study and a summary of the literature review that was conducted. Field methods used in the project are described in Sec. 3. Sec. 4 describes the field data that were obtained and how the data were incorporated into the model. Sec. 5 contains a summary and conclusions. Recommendations are presented in Sec. 6.

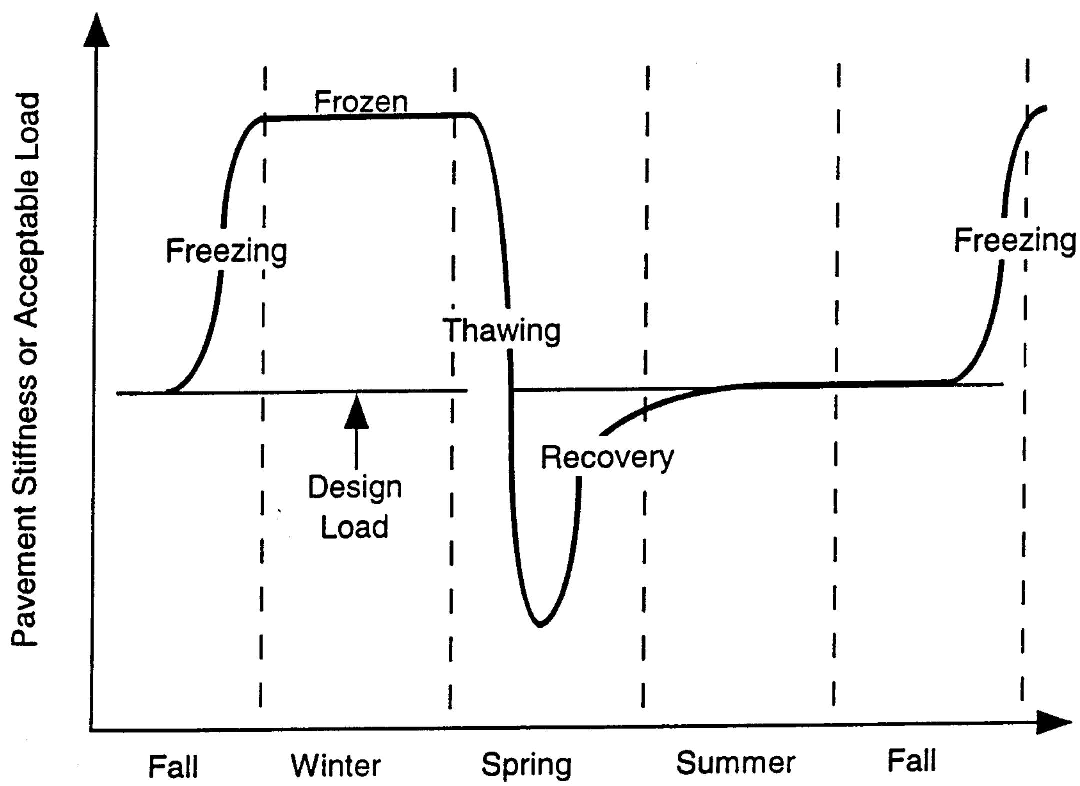

Fig. 1.1. Seasonal variation of pavement stiffness or acceptable load.

SECTION 2
BACKGROUND

2.1 PURPOSE AND OBJECTIVES OF STUDY

The Wisconsin Department of Transportation (WisDOT) is responsible to the citizens of Wisconsin for providing quality transportation systems throughout the year. Part of this responsibility involves the modification of load limits placed on highways throughout the state during the year to prevent excess road damage. During the months of June through November, normal load limits are placed on all roads, restricting loads to a maximum of 36,000 kg. However during the months of December through May different load restrictions may be invoked depending on whether the road is frozen, thawing, or recovering.

Three regulations are used to restrict load limits: (1) the frozen road declaration (mid Dec. to mid March), (2) spring weight restrictions on Class 2 highways (mid March to mid May), and (3) posted road load limits. WisDOT personnel use weather data, frost tube and road cell data, and experience to determine the timing of these load limit regulations. Weather data are used to estimate when to issue the frozen road declaration and when spring load limits should be issued or posted. In some cases, an FHWA method is used in conjunction with weather data to predict when thaw weakening will occur. The frost tube system began about 20 years ago but is currently seeing less use because it requires that WisDOT personnel regularly examine the frost tubes. Data collected from 29 "road cells," which are part of the Wisconsin Winter Weather system, are also used to assess whether pavement subsoils are frozen or thawing. A "road cell" is a pavement section where meteorological data are recorded and temperatures at the pavement surface, 45 cm down, and 90 cm down are monitored.

WisDOT believes that the current methods used to determine the timing of weight restrictions on state highways are ill-defined, inadequate, and non-uniform. Placing excess loads on a roadway when its structure is in a weakened state can cause loss of pavement life, increased maintenance costs, loss of service to customers, and affect economic development. Consequently, WisDOT desired to critically assess the methods currently being used and to develop new methodology based on hard data that will permit WisDOT personnel to accurately determine the timing of load limit restrictions. This project was conducted to fill this need. The particular objectives were:

- Develop a methodology based on hard data to cost effectively and efficiently determine the timing of weight restrictions on state highways.

- Assess effectiveness of current available techniques including frost tubes, road cells, gravedigger data, utility crews, etc.

- Develop a method that is compatible with the Wisconsin Winter Weather System (W3S), if possible.

The first two objectives were met in this project. The third objective could not be met because of incompatibility of the software and hardware used to operate W3S.

The project consisted of four tasks. Task 1 consisted of a comprehensive literature survey. The results of this survey are described in Yesiller et al. (1995) and Jong (1997). Task 2 consisted of an analysis of existing data. Results of this task are described in Yesiller et al. (1995). Task 3 consisted of instrumenting three sites in Wisconsin for monitoring meteorological conditions, subsurface thermal conditions, and pavement stiffness. Collection and analysis of the monitoring data were conducted in Task 4. In Task 5, a model was developed based on the data that were collected. The results of Tasks 3 and 4 are described in this report. Bosscher et al. (1998) describe the model developed in Task 5.

2.2 LITERATURE SEARCH SUMMARY

Thaw weakening is a function of the type of soil, the pavement structure and thickness, water content of the base and subgrade, and the depth of frost penetration. Significant reductions in pavement stiffness during thaw periods are widely recognized as a major source of pavement damage. As a result, many investigators have studied thaw weakening and have attempted to establish criteria and procedures for applying load restriction practices during the spring thaw period.

The literature reveals that many different criteria have been proposed for weight restrictions during thawing, whereas practically no information exists regarding timing of permissible overloads. Some procedures are based on air temperature while others are based on frost depth or related factors. Existing criteria for determining when weight restrictions should be imposed are summarized as follows:

- when the top of base course starts thawing (McBane and Hanek 1986, Janoo and Berg 1990)
- when the bottom of base course starts thawing (Rutherford and Mahoney 1986 FHWA 1987)
- when the thaw index is -1.1 to 10 °C-days based on a 0°C-reference temperature (Mahoney 1985)
- when deflections are > 45 to 50% of summer deflection values (Rwebrangira et al. 1987)
- when the thaw depth is 10 to 20 cm below the pavement surface (Thomassen and Eirum 1982)

Criteria that have been suggested for timing the termination of load restrictions are summarized as follows:

- when the pavement is completely thawed (Scrivner 1969, Rutherford and Mahoney 1986, FHWA 1987)
- when the thaw depth is 120 cm (McBane and Hanek 1986)
- when a specified period after the "critical thaw depth" has been reached (Thomassen and Eirum 1982)

Suggested load reductions during the thaw-weakening range from 25% (Thomassen and Eirum 1982) to 60% (Mahoney at el. 1985) of the allowable summer load.

Review of the literature also shows that the criteria used for load restrictions during the spring thaw period are poorly defined and non-uniform. Some criteria are even contradictory. For example, the FHWA guidelines suggest that load restrictions can be removed when the pavement is completely thawed, whereas other studies have shown that the pavement is its weakest condition when the pavement is completely thawed (Nordal 1982, Janoo and Berg 1996). Consequently, there is a need to determine when the critical periods are in terms of pavement distress, and to develop a rational procedure for predicting when these critical periods occur. Moreover, a rational method needs to be developed to predict acceptable loads during these critical periods.

SECTION 3
RESEARCH METHODOLOGY

3.1 FIELD SITES

Three sections of secondary highways were selected for monitoring pavement performance and subsurface conditions. Locations of the sites are shown in Fig. 3.1. Two sites were located in northern Wisconsin along County Road F near Unity, Wisconsin and State Highway 102 near Spirit, Wisconsin. The third site was located in western Wisconsin on the frontage road for Highway 27 near Westby, Wisconsin. Detailed locations of the sites are shown in Figs. 3.2 and 3.3. These sites are referred to herein as Unity, Spirit, and Westby.

The pavement structure at each site was observed when excavating a trench for installing subsurface instrumentation. Profiles for each site are shown in Fig. 3.4. At Westby, the pavement is primarily a 36-cm-thick base course of good quality crushed stone overlain by a thin asphalt layer about 0.4 cm thick. The subgrade is lean silty clay. At Unity, the asphalt concrete layer is 31 cm thick and the base course is 23 cm of sand with a trace of gravel. The subgrade consists of two strata. The upper layer is gray lean silty clay with a thickness of 74 cm. Underneath is a layer of brown sandy clay. At Spirit, the asphalt concrete layer is 34 cm thick and consists of several asphalt concrete overlays. The base course is 37 cm thick and consists of silty sand with gravel. A silty to clayey sand subgrade is beneath the base course.

3.2 FIELD INSTRUMENTATION

3.2.1 Meteorology

Meteorological data collected at all field sites included ambient air temperature, relative humidity, solar radiation, wind speed, and wind direction. This information is used in the thermal modeling for predicting freeze and thaw depths. The instruments employed for each measurement are summarized in Table 3.1.

Table 3.1. Instruments used for meteorological measurements

Meteorological Measurement	Instrument	Output Signal
Air Temperature	Thermistor	Resistance (excitation with voltage measurement)
Relative Humidity	Capacitive relative humidity sensor	Excitation with voltage measurement
Solar Radiation	Silicon pyranometer	Low level voltage (12 mV max.)
Wind Speed	Anemometer	Low level ac signal (frequency proportional to wind speed)
Wind Direction	Potentiometer wind vane	Resistance (excitation with voltage measurement)

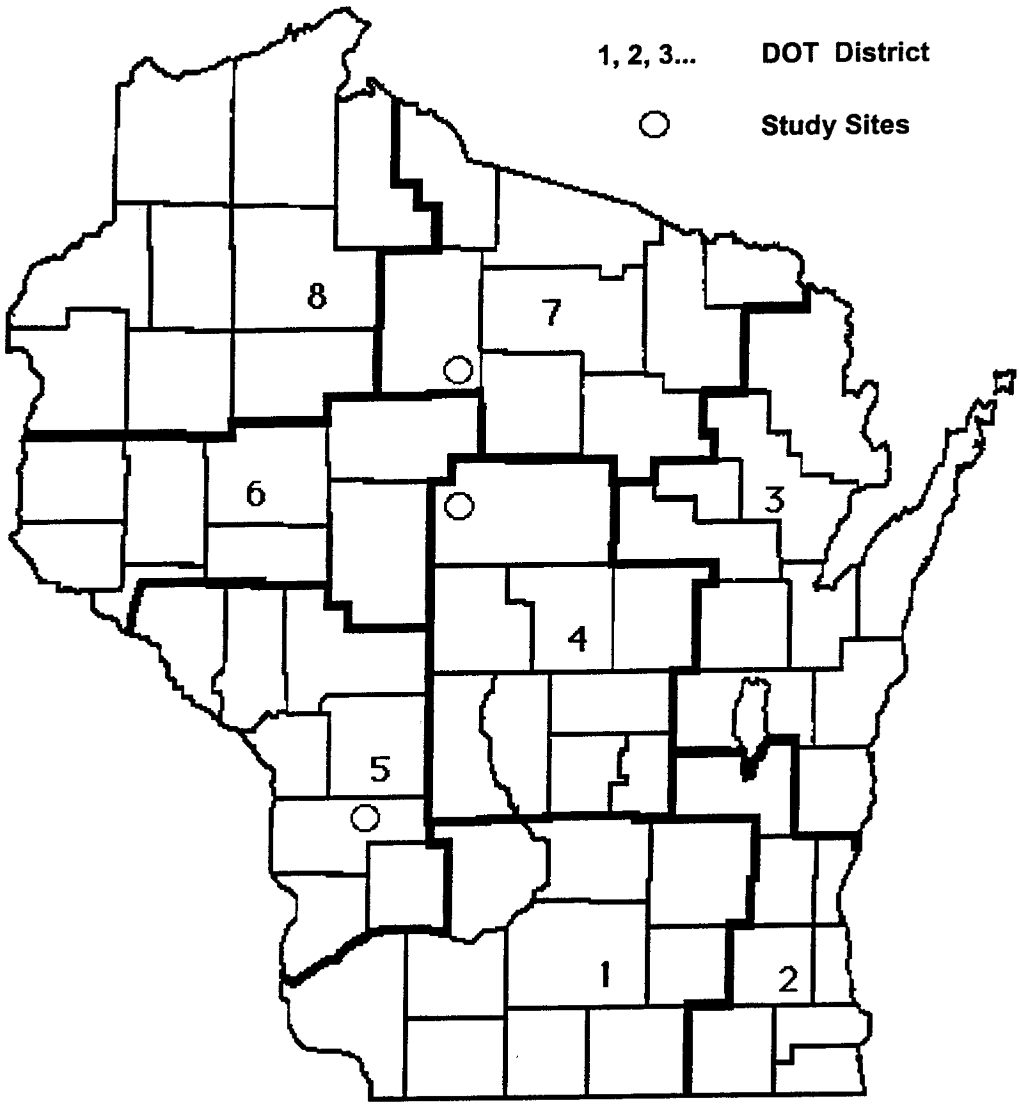

Fig. 3.1. Locations of field sites.

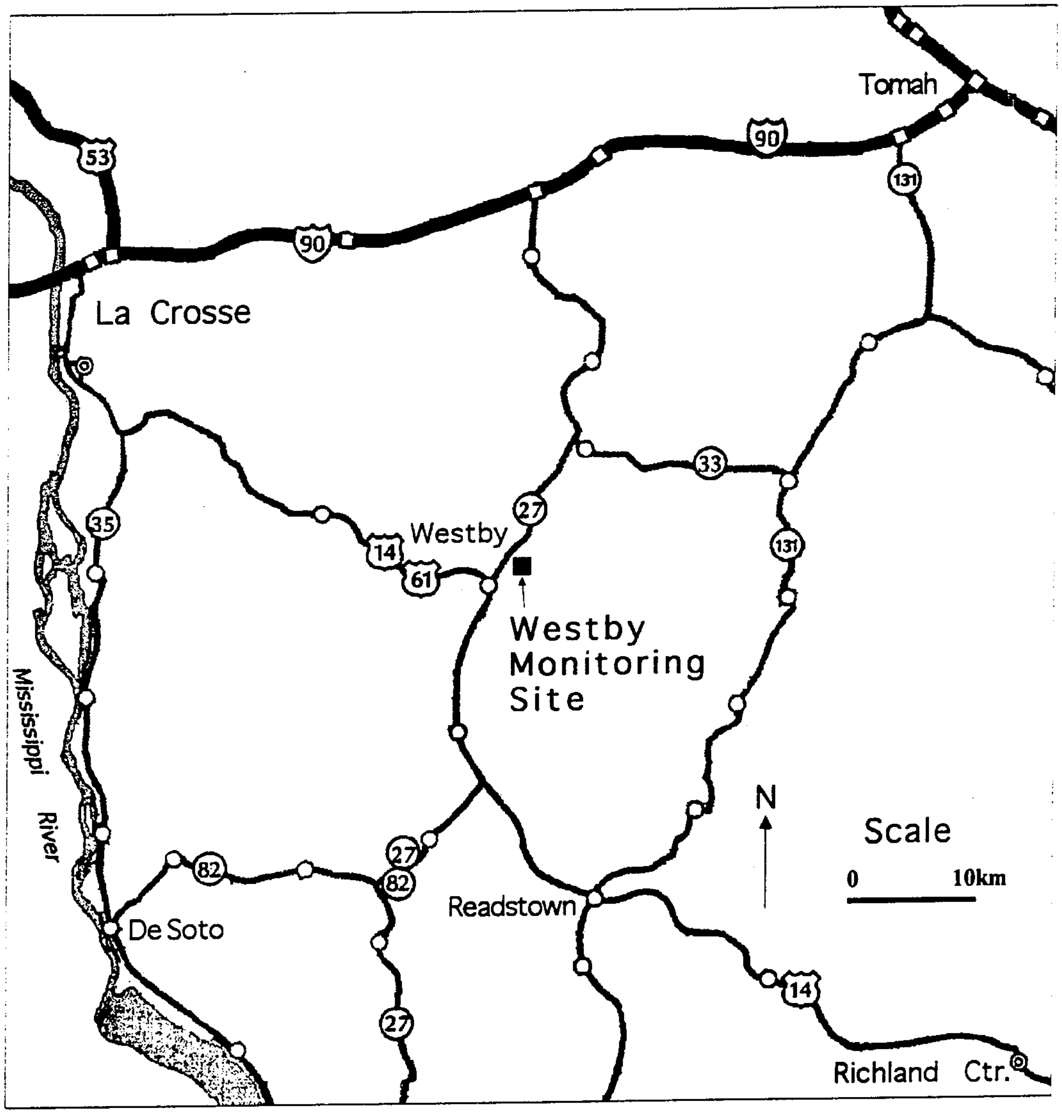

Fig. 3.2. Location of Westby site.

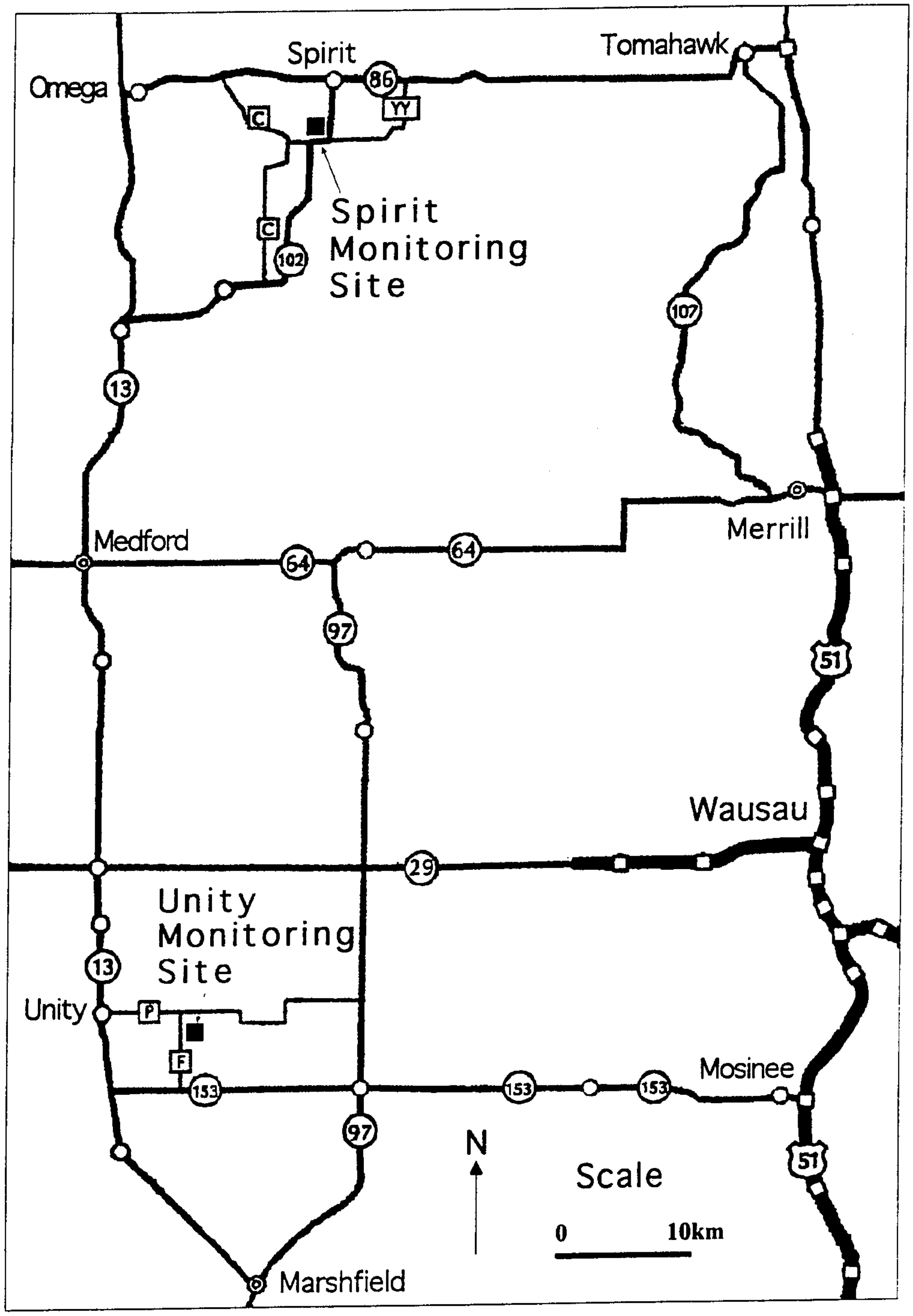

Fig. 3.3. Locations of Unity and Spirit sites.

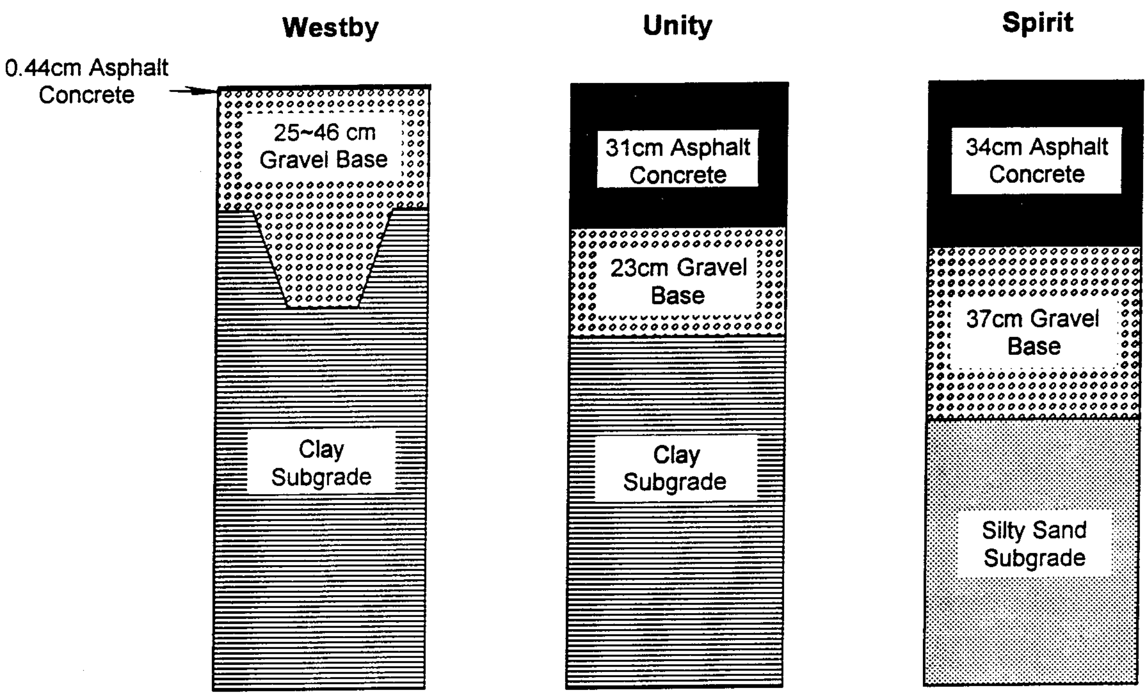

Fig. 3.4. Pavement structures.

3.2.2 Subsurface Monitoring

Subsurface data that were collected included temperature, water content, and dielectric constant, the latter being used to determine when the pore water changed phase. The data were used in the thermal modeling and to determine freeze and thaw depths when analyzing pavement stiffness.

Soil temperature was measured with thermistors and thermocouples at each site. Both devices were used because consensus does not exist in the scientific community regarding which device is more reliable when measuring soil temperature (Barcomb 1989, Rada et al. 1995). Using both sensors provided assurance that reliable data were collected. In addition, installing additonal sensors required little effort or expense.

Time domain reflectometry (TDR) was used to measure water content and dielectric constant of the base and subgrade. In the TDR technique, the travel time of an electromagnetic pulse traveling through soil is measured. A metallic cable tester (Tektronix 1502B) is used to send and receive the electromagnetic pulses to TDR probes embedded in the subsurface.

The travel time is used to determine the apparent dielectric constant (K_a), which is primarily a function of the volumetric water content (θ). The dielectric constant of air is 1, whereas the dielectric constant of soil solids is typically between 3 and 5 depending on the soil type and dry density. The dielectric constant of liquid water is about 80 (Topp et al. 1980), whereas it is about 3 for ice. Because the dielectric constant of water is much greater than that of soil solids, ice, and air (about 80, 4, 3, and 1, respectively), the dielectric constant of water dominates the apparent dielectric constant of soil even at low water content. Thus, changes in volumetric water content or changes in phase result in a change in the apparent dielectric constant of the soil.

The unfrozen volumetric water content is inferred from a calibration curve relating apparent dielectric constant and volumetric water content. Research has shown that the relationship between volumetric water content and apparent dielectric constant is not greatly affected by soil type, unless the soil is moderately plastic clay. Thus, a single calibration curve can be used for a variety of soils without significant error. Several calibration equations have been reported. Topp et al. (1980) proposed the following equation relating K_a and θ:

$$\theta = -5.30 \times 10^{-2} + 2.92 \times 10^{-2}K_a - 5.5 \times 10^{-4}K_a^2 + 4.3 \times 10^{-6}K_a^3 \qquad (3.1)$$

Smith and Tice (1988) proposed a separate calibration equation for frozen soils:

$$\theta = -1.458 \times 10^{-1} + 3.868 \times 10^{-2}K_a - 8.502 \times 10^{-4}K_a^2 + 9.920 \times 10^{-6}K_a^3 \qquad (3.2)$$

The K_a-θ relationship for frozen soil is generally a function of soil type and depends on the water content prior to freezing. Thus, Eq. 3.2 cannot be generally applied to all soils. In this study, only Topp's equation (Eq. 3.1) was used. Consequently, water contents reported for frozen soil are not the true unfrozen water contents.

3.2.3 Data Collection and Control System

The variety of information and the frequency of measurements made at each site required that an automated data acquisition and control computer be used for controlling the instrumentation and storing the data. In this study, a CR10 measure-and-control module [Campbell Scientific, Inc. (CSI)], more commonly referred to as a datalogger, was used along with associated equipment manufactured by CSI. The datalogger controls the data acquisition hardware and records data from each of the sensors. A two-hour time interval was used for collecting data in this project. The storage capacity of the CR10 datalogger was large enough to store about one month of data.

Several other pieces of equipment were also used. Multiplexers switched the TDR, thermistor, and thermocouple probes so that multiple measurements could be made through a single connection with the datalogger. A cellular transceiver and modem were installed at each site for telecommunications and to down load data to a computer at the University of Wisconsin-Madison. Two 12-volt batteries (Delco Voyager automotive batteries) were used at each site as the power source, one for the measurement system and the other for the telecommunication system. Two solar panels were used at each site to recharge the batteries.

3.2.4 Installation of Monitoring System

A trench approximately 0.75 m wide and 2.0 m deep was excavated at each site for installation of the instrumentation. Each trench was oriented perpendicular to the alignment and extended across one lane (from centerline to shoulder). The thermistors, thermocouples, and TDR probes were inserted at various depths into one side of the trench directly between the wheel paths. All sensors were placed horizontally. The arrangement of the sensors is illustrated in Fig. 3.5. The horizontal spacing between the sensors was about 15 cm. Locations of the sensors at each site are summarized in Table 3.2.

After the sensors were installed, the trenches were backfilled in lifts and compacted with a jumping-jack compactor. Hot mix asphalt was then used to re-pave the top surface. During the backfilling process, efforts were made to re-build each pavement structure as closely as possible to its original geometry and condition. Care was also used to ensure that the sensors and cables were not damaged or detached during backfilling.

Table 3.2. Locations of sensors installed at study sites.

	Depth of sensors below surface (cm)		
Sensor	Westby	Unity	Spirit
Thermocouple	8, 15, 23, 30, 38, 46, 61, 76, 91, 122, 152, 183	30, 38, 46, 53, 61, 69, 76, 84, 91, 99, 107, 114, 122, 130, 137, 145, 152, 160, 168, 175, 183	34, 42, 50, 57, 65, 72, 80, 88, 95, 103, 110, 118, 126, 133, 141, 149, 156, 164, 171, 179
Thermistor	15, 30, 46, 61, 76, 91, 122, 152	46, 61, 76, 91, 107, 122, 152, 183	50, 65, 80, 95, 110
TDR	15, 30, 46, 61, 76, 91, 122, 152	46, 61, 76, 91, 107, 122, 152, 183	50, 65, 80, 95, 110, 126, 156, 187

Cables and wires from the sensors were routed through a 10-cm-diameter PVC pipe. The pipe extended from the bottom of the trench and out to equipment cabinets

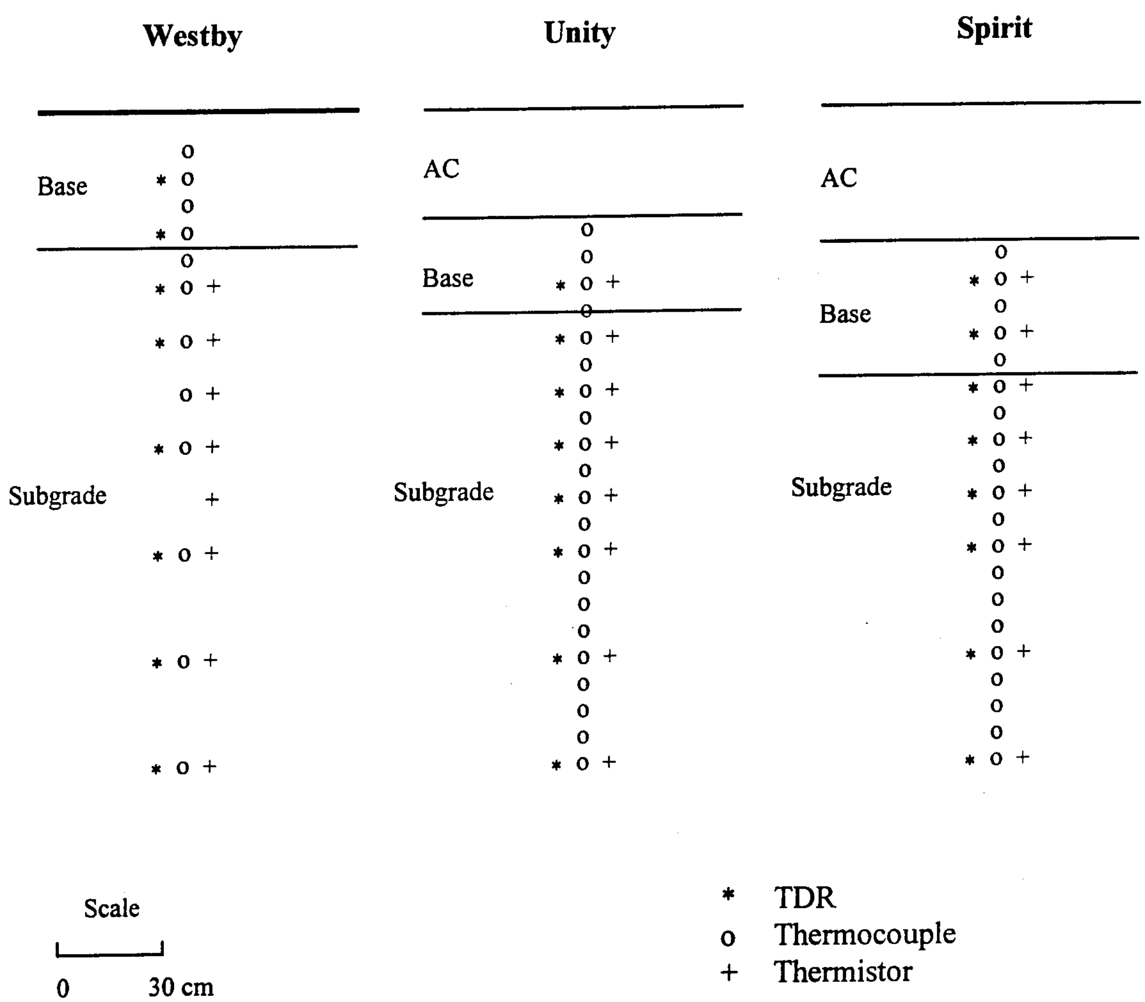

Fig. 3.5. Locations of subsurface sensors.

located about 2 m from the shoulder. Two steel pipes were pounded vertically into the ground to support the equipment cabinets, which housed the datalogger, cellular modem and transceiver, TDR cable tester, multiplexer, and other instruments. A schematic of a typical instrumentation layout is shown in Fig. 3.6 and a photograph of the layout at Unity is shown in Fig. 3.7.

3.3 MEASURING PAVEMENT MODULI

3.3.1 Falling-Weight Deflectometer

A KUAB 2-m falling weight deflectometer (FWD) (model 2m-33) was used for collecting the deflection data needed for determining the moduli of the pavement layers. Key features of the KUAB 2m-FWD device are summarized in Table 3.3.

Table 3.3. Key features of the KUAB 2m-FWD.

Features	KUAB 2m-FWD
Load range	14-150 kN
Load rise time	17-25 msec
Load duration	34-50 msec
Standard drop test sequence	35 sec
Load generator	Two mass system
Load plate	300-mm-diameter segmented plate
Number of sensors	9
Deflection sensor	Seismometer
Deflection sensor position	0 - 180 cm
Deflection resolution	1 μm
Absolute accuracy	better than 2% of indicated reading
Test sequence	Unlimited, user specified

Fig. 3.8 shows the KUAB 2m-FWD device, which was supplied by WisDOT. The KAUB 2m-FWD is a trailer-mounted device that is towed by an automobile. A computer in the towing vehicle controls the FWD. Deflections and other data are recorded and stored in the computer.

The KUAB 2m-FWD creates an impulse force by means of a combined two-mass and buffer system. A schematic of the two-mass loading mechanism is shown in Fig. 3.9. A photograph is shown in Fig. 3.10. The two masses are referred to as the falling weight and the intermediate weight. Unlike other FWDs, in which the falling weight is dropped directly on the loading plate resting on the pavement surface, the KUAB 2m-FWD drops the falling weight first on an intermediate mass and then the force is transmitted to a segmented loading plate. The purpose of the segmented loading plate is to generate a more reproducible load pulse and to better simulate the load pulse created by a moving wheel.

Surface deflections are measured with nine velocity transducers (Fig. 3.10), which use a mass-spring system and a linear voltage differential transformer (LVDT) as the distance-sensing element. Velocity transducers are also known as seismometers or geophones. Each geophone has a range of 5 mm, and is permanently mounted on a micrometer screw for static calibration.

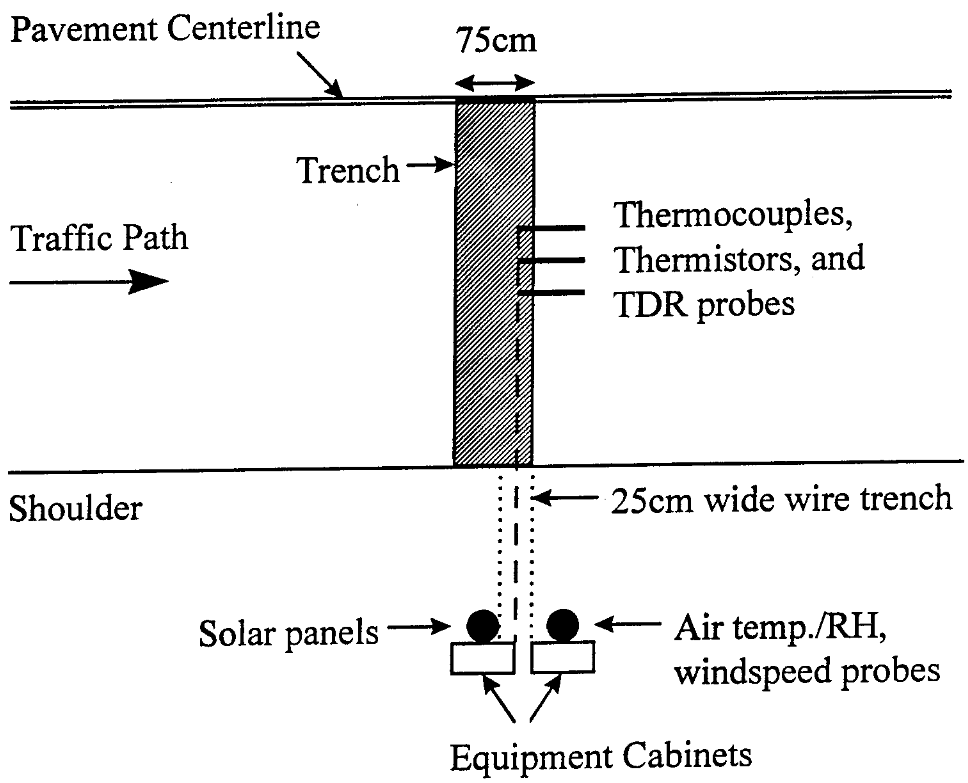

Fig. 3.6. Typical instrumentation layout.

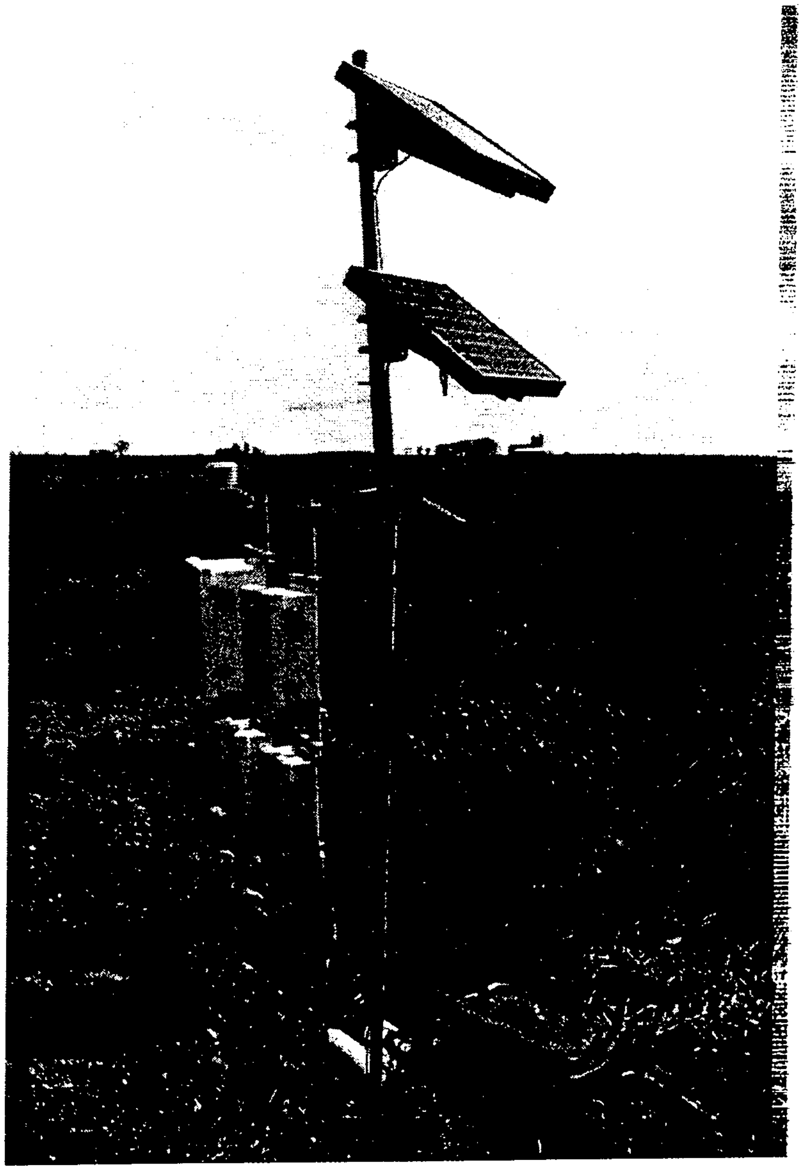

Fig. 3.7. Field monitoring system at Unity.

Fig. 3.8. The KUAB 2m-FWD.

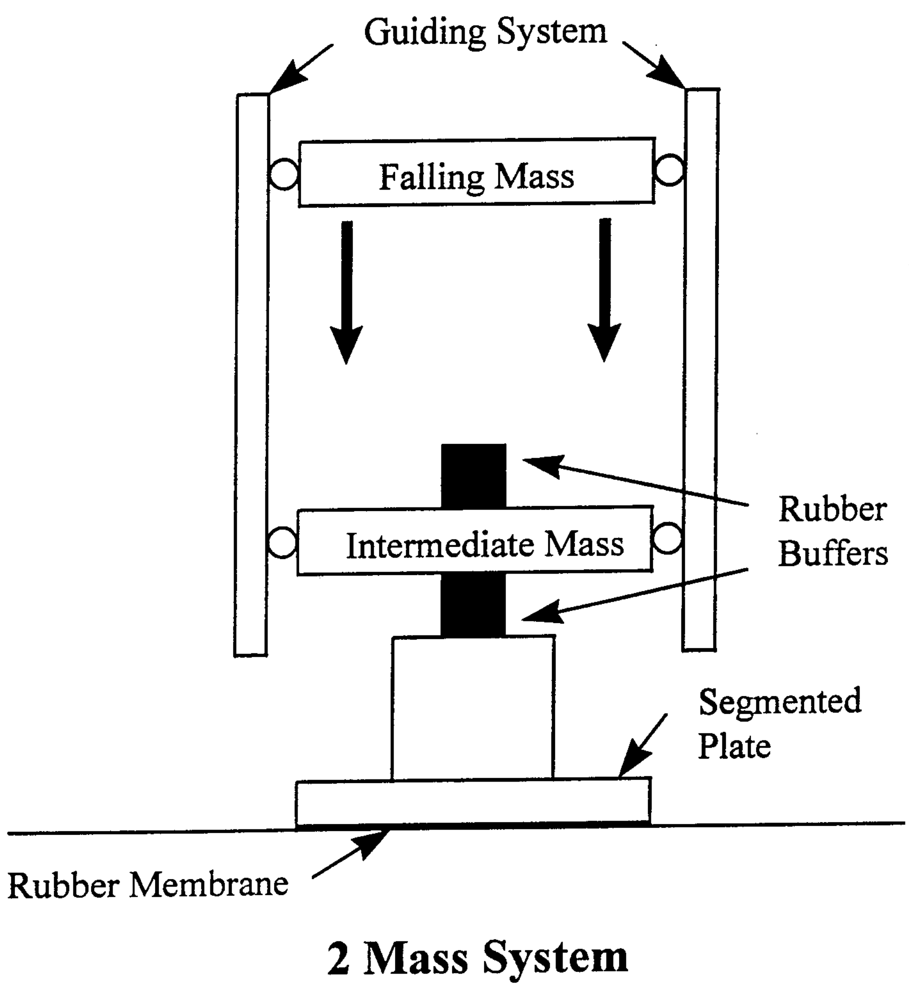

Fig. 3.9. Schematic of the two-mass loading mechanism.

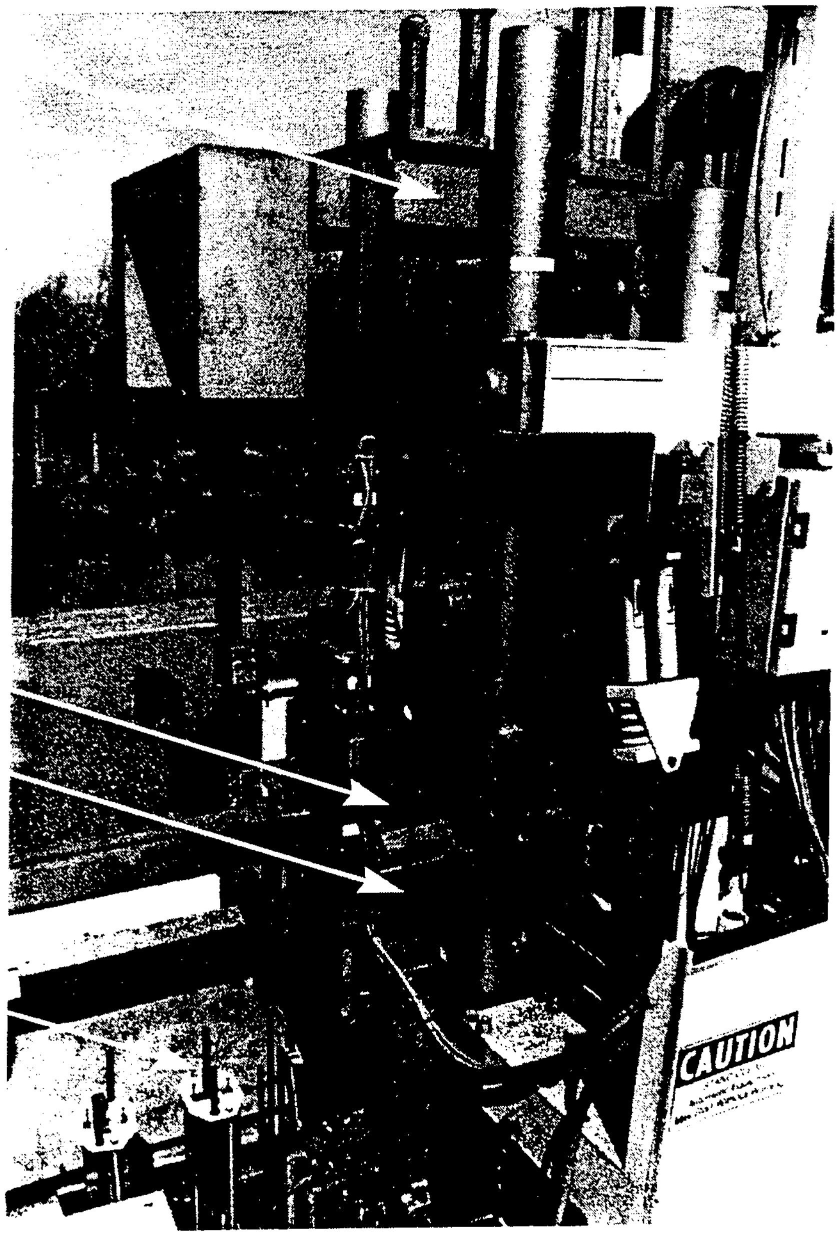

Fig. 3.10. The two-mass loading system.

3.3.2 Backcalculation of Moduli

Moduli of the pavement layers were back-calculated from the deflection data collected with the FWD using the MODULUS program developed by the Texas Transportation Institute (TTI 1991). Rules described in SHRP (1993) were used in the back-calculation analysis.

Even though the SHRP guidelines were followed, some assumptions were necessary. At Westby, a thin (0.4-cm) layer of AC exists. For such layers, the SHRP guideline recommends that the modulus be fixed at a reasonable value or that the layer be incorporated into an adjacent layer. In this study, the modulus of the thin AC layer was fixed at a constant value estimated using the Asphalt Institute equation (Jong 1997) and the pavement temperature measured with the FWD during testing. At Unity, the two subgrade layers are both clays, and thus they were combined into a single layer during backcalculation process. The observed pavement profile was used without modification at the Spirit site.

A stiff layer was introduced at depth at each site using the algorithm employed by the MODULUS program, which follows the procedure described in Uzan (1994). Estimates of subgrade thickness based on the depth to the stiff layer predicted by MODULUS are shown in Fig. 3.11 for the Unity and Spirit sites. In effect, a thicker subgrade corresponds to a deeper stiff layer. The depth of the stiff layer is not constant, but varies with time. In particular, the stiff layer becomes deeper as the pavement becomes stiffer in winter and shallower in the spring when the pavement is softer. In some cases during the spring thaw, MODULUS predicted that the stiff layer was located within the AC layer or the base course, which is impossible. Thus, the depth to the stiff layer estimated by MODULUS could not be used for all seasons. Experience with the program showed, however, showed that a stiff layer was necessary to obtain realistic moduli (Jong 1997).

Because the depth to the stiff layer was practically constant during the summer (Fig. 3.11), and during this period the pavement stiffness is not affected by environmental stress, the depth of the stiff layer obtained during the summer was assumed to be representative for the entire year. In particular, the depth of the stiff layer was set at 735 cm for Westby, 206 cm for Unity, and 135 cm for Spirit. Use of these stiff layer depths resulted in 5% to 10% total absolute error, which the authors believe is reasonable and acceptable.

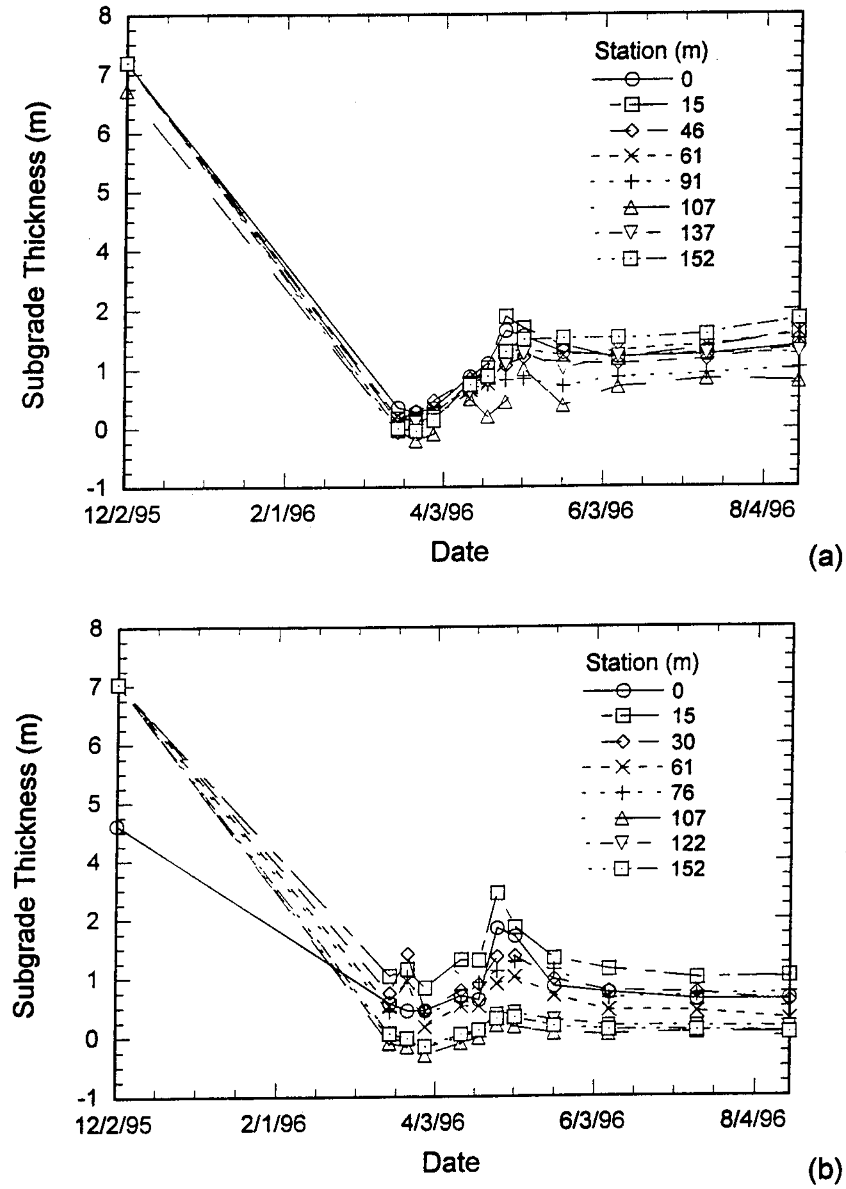

Fig. 3.11. Thickness of subgrade predicted by MODULUS: (a) Unity, (b) Spirit.

SECTION 4
FIELD DATA

4.1 METEOROLOGICAL DATA

The monitoring program began in November 1995 and ended in June 1997. Meteorological data collected during this period were primarily used to calibrate the one-dimensional heat transfer code (MUT1D) used in the model. Samuelson and Benson (1997) calibrated MUT1D as part of this study. This section briefly describes how reliability of the data was checked, and provides examples of typical data collected in 1995-96 from Spirit. Meteorological records for each site are in the Appendix.

4.1.1 Reliability

To assess the reliability of the on-site meteorological data, additional data were collected from nearby weather stations operated by the National Weather Service (NWS). The NWS weather stations are located at Viroqua, Owen, and Hurley, Wisconsin. Typical comparisons of the data collected on-site and by the NWS are shown in Fig. 4.1. Only the on-site daily mean air temperatures are shown for clarity. The on-site daily air temperatures fall between the daily maximum and minimum temperatures reported by the NWS, suggesting that the field data are reliable. Similar comparisons were obtained for the other measurements.

4.1.2 Typical Meteorological Conditions

Meteorological data collected at Spirit are presented in this section to illustrate conditions existing in northern Wisconsin during the monitoring period. Data for all sites are in the Appendix.

Average daily air temperature at Spirit is shown in Fig. 4.1. During Winter 1995-96, the daily average air temperature was typically about -10°C, whereas the average daily air temperature was about 20°C the following summer. These temperatures are characteristic of typical conditions in northern Wisconsin. Relative humidity data are shown in Fig. 4.3. The relative humidity typically fluctuated between 50 to 90%. Somewhat drier and more variable conditions exist during Spring. The relative humidity is least variable during the Fall (about 85%).

Solar radiation is shown in Fig. 4.4. Solar radiation is highest during the summer, and least during the winter. The average daily solar radiation received during the summer is about 250 W/m^2, which is characteristic of states in the northern tier of the United States. During the fall and winter seasons, solar radiation is typically about one-third of the summer value.

Wind speed data are shown in Fig. 4.5. The highest wind speeds occur during the winter. The typical average wind speed in winter is about 3.5 m/sec, but average values as high as 7 m/sec were measured. During summer, the winds are milder, with the average wind speed being about 2.0 m/sec.

4.2 SUBSURFACE DATA

Water content, temperature, and dielectric constant were measured in the base and subgrade at each site. There are some periods for which data are missing due to

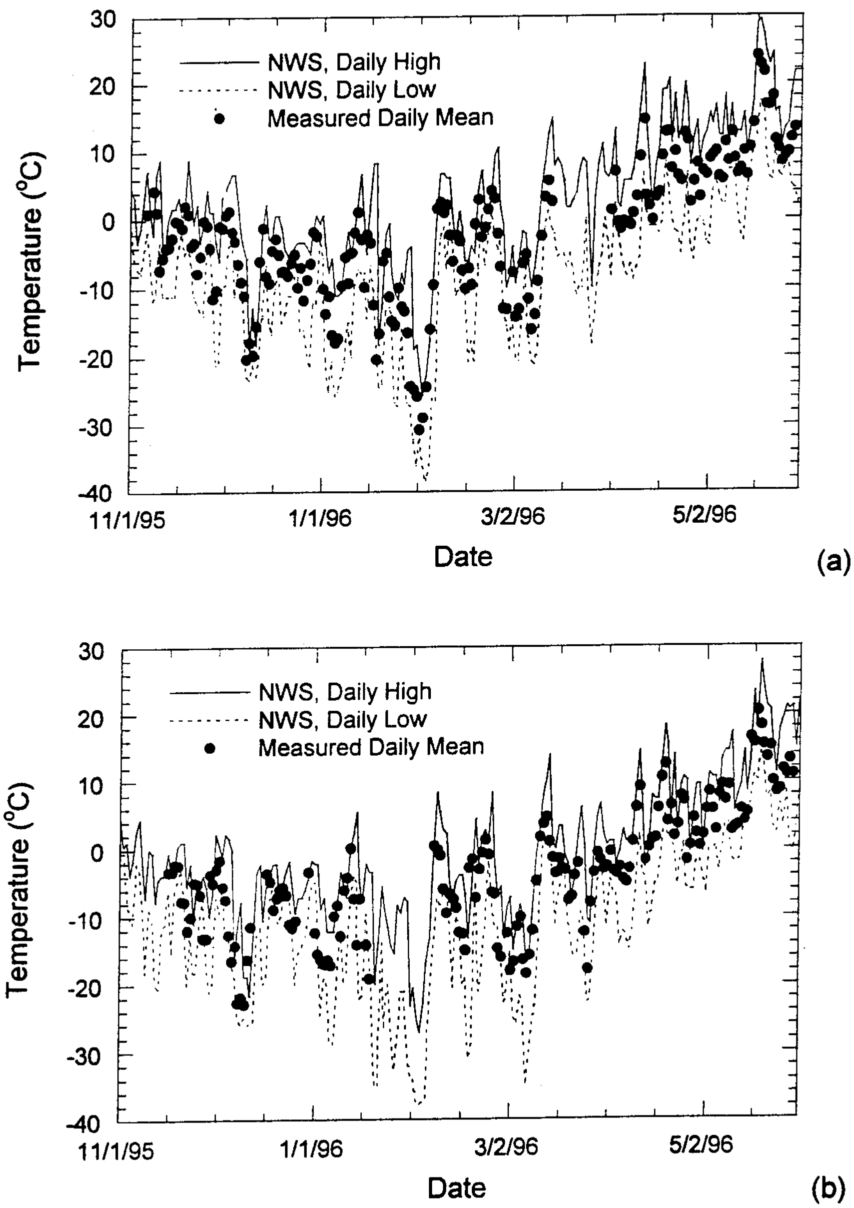

Fig. 4.1. Comparison of on-site and NWS air temperature at (a) Westby and (b) Unity.

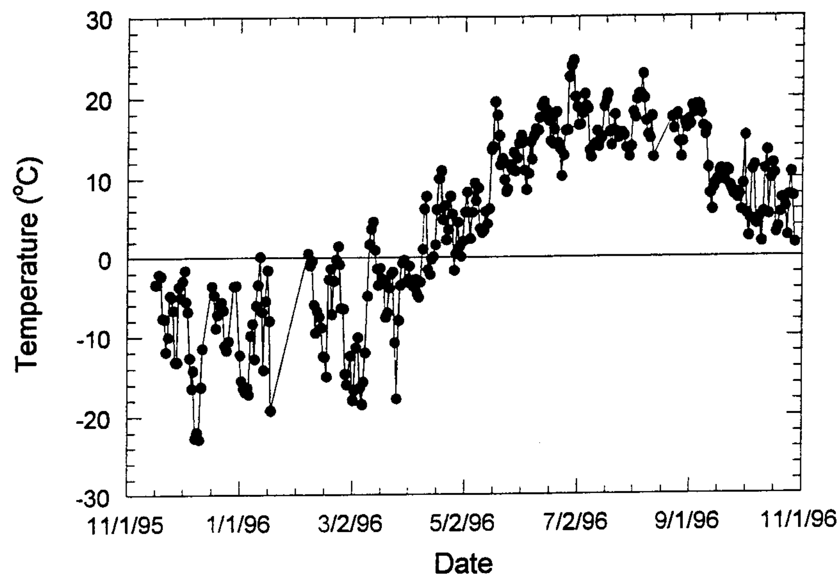

Fig. 4.2. Daily average air temperature at Spirit.

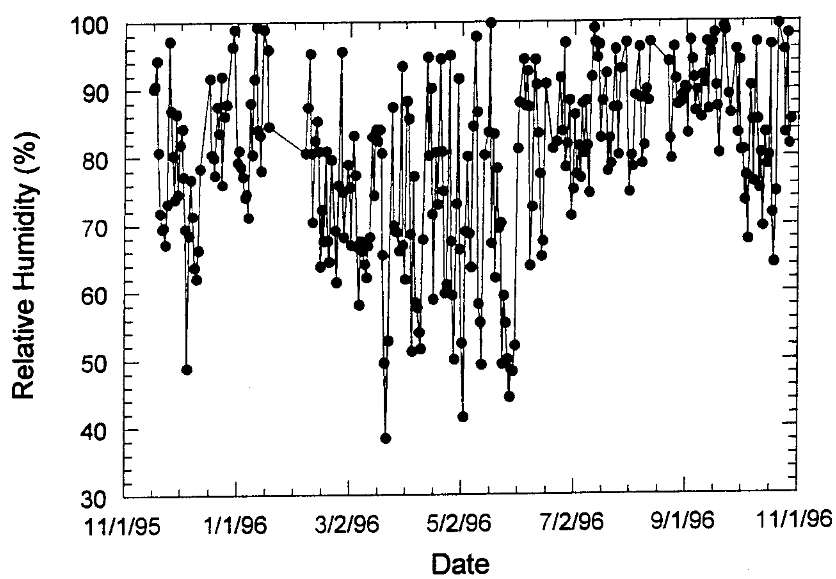

Fig. 4.3. Daily average relative humidity at Spirit.

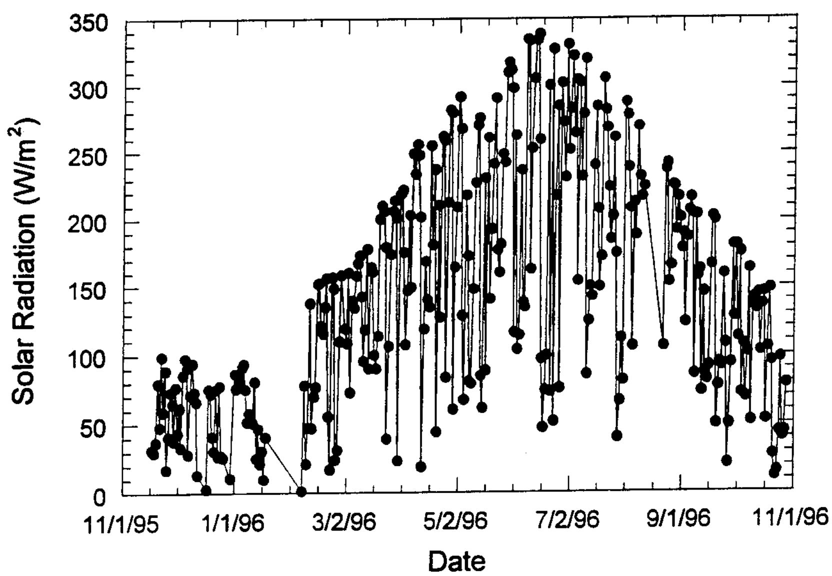

Fig. 4.4. Daily average solar radiation at Spirit.

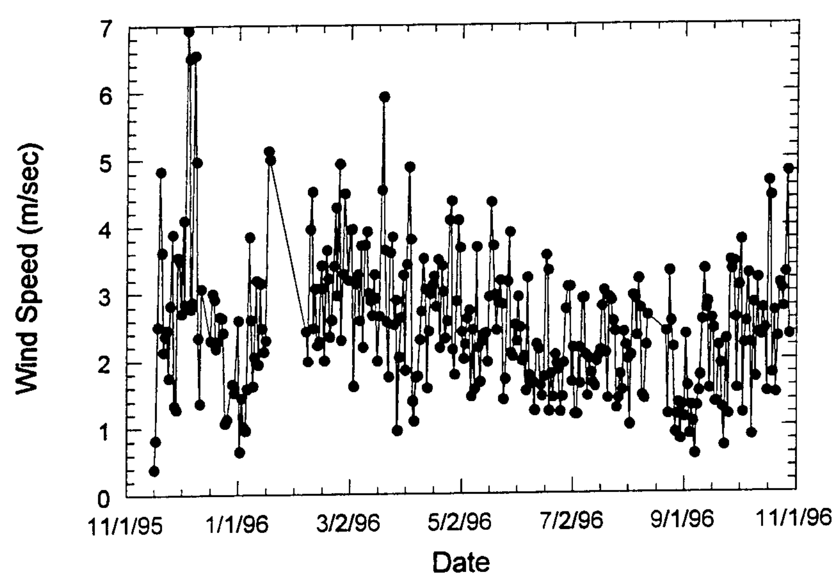

Fig. 4.5. Daily average wind speed at Spirit.

battery failures. However, a general record of subsurface conditions exists for all sites.

4.2.1 Volumetric Water Content

Volumetric water contents for Westby, Unity, and Spirit are shown in Figs. 4.6 - 4.8 for the 1995-1996 fall-spring period. Similar data were obtained in 1996-1997. At each site the water contents drop suddenly at all depths in late fall and then increase suddenly each spring. These sudden changes in water content correspond to freezing and thawing of the pore water, which result in a dramatic change in the volume of liquid water in the soil. The water contents after thawing are usually higher than before freezing as a result of water that accumulated as ice within the soil during the winter. This is particularly true of the base course, which appears to be nearly saturated after thawing (e.g., Fig. 4.9 for Spirit), whereas it has fairly low water content before freezing. Shortly after thawing is complete, the water contents in the base begin to decrease as the base and subgrade drain (Fig. 4.10).

4.2.2 Soil Temperature

4.2.2.1 Thermocouples vs. Thermistors

Installation of thermocouples and thermistors at each site allowed a comparison of temperatures measured using both devices. Soil temperatures measured with thermocouples and thermistors at a depth of 66 cm at Spirit are shown in Fig. 4.11. The temperatures measured with both devices are nearly identical. Data from the same set were used to create a graph of temperature measured with thermistors vs. temperatures measured with thermocouples, as shown in Fig. 4.12. For a wide range of temperatures (-7°C to 26°C), essentially the same temperature was obtained by both devices. The data fall along a 1:1 line and are virtually devoid of scatter. Similar results were obtained for different depths and at different sites, suggesting that either device is equally valid for measuring soil temperature.

4.2.2.2 Soil Freezing and Thawing Temperature

The freezing point of the base and subgrade are needed for use in MUT1D. Generally, the freezing point of base and subgrade materials is less than 0 °C due to the effects of matric suction and soluble salts (Leonards and Andersland 1960). To determine representative temperatures of phase change for the base and subgrade materials in this study, soil temperatures from each site were compared to dielectric constants measured simultaneously with TDR. As mentioned in Sec. 3.2.2, the dielectric constant of moist soil changes dramatically when the soil freezes because the dielectric constant of the pore water decreases from about 80 when unfrozen to 3 when frozen.

Dielectric constant vs. soil temperature is shown in Fig. 4.13 for freezing and thawing conditions at Westby. The data were collected from a depth of 91 cm. The dielectric constant changes dramatically as the soil temperature approaches 0°C. In particular, when the soil is unfrozen the dielectric constant is about 25 whereas it is about 10 when the soil freezes. Examination of Fig. 4.13b shows that freezing of the soil begins when the temperature is about -0.2°C. The soil also appears to thaw at -0.2°C. Similar graphs for Unity and Spirit are shown in Figs. 4.14 and 4.15. At Unity, the freeze-thaw temperature is about -0.3 to -0.4°C and at Spirit it is about -0.7°C.

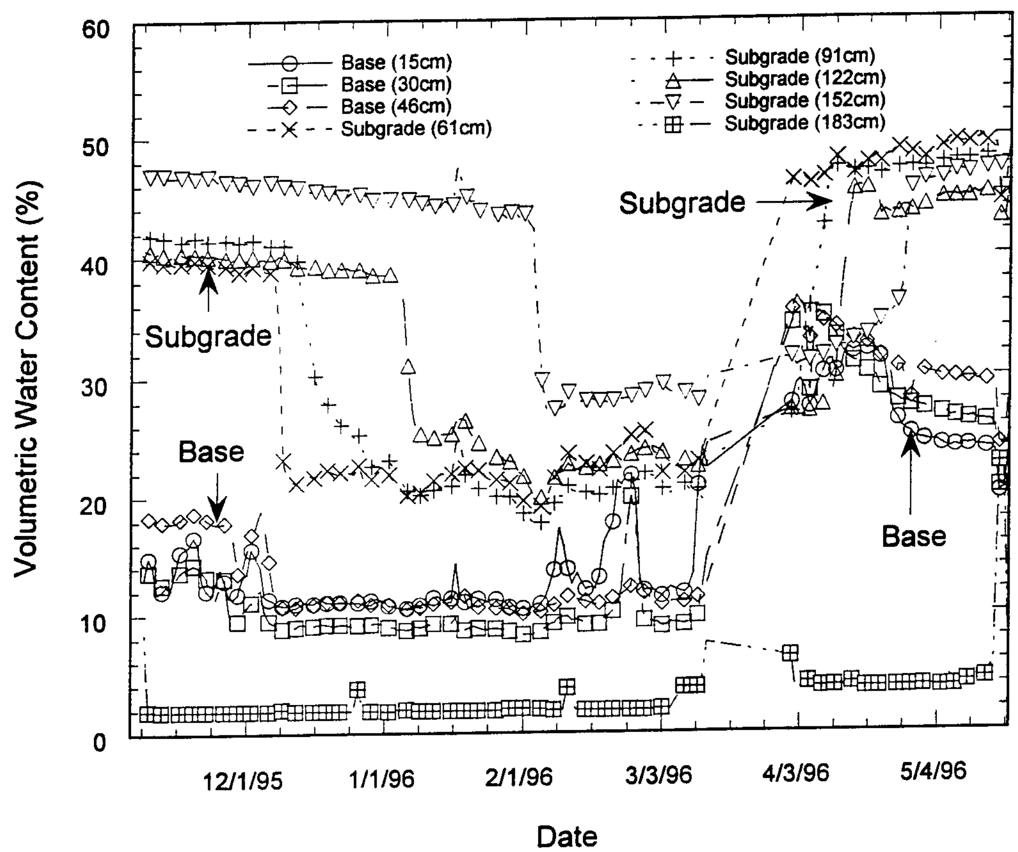

Fig. 4.6 Volumetric water contents at Westby.

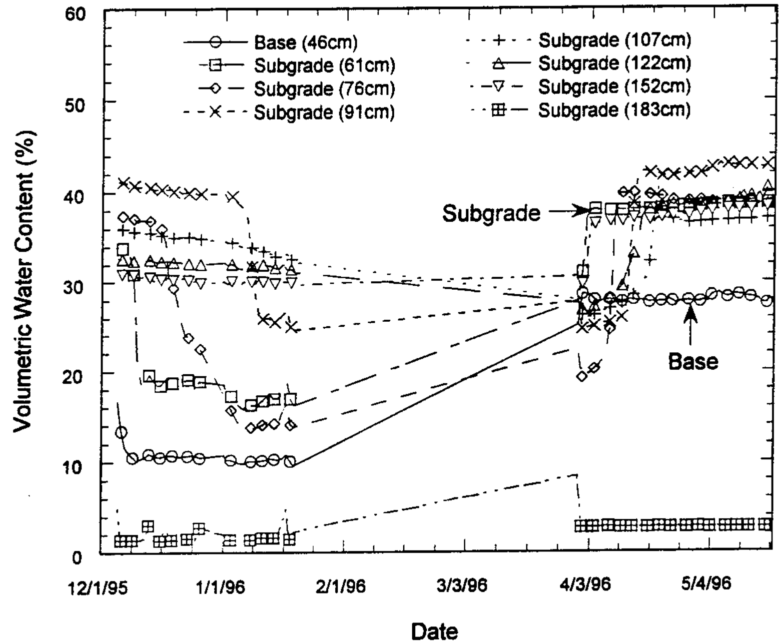

Fig. 4.7. Volumetric water contents at Unity.

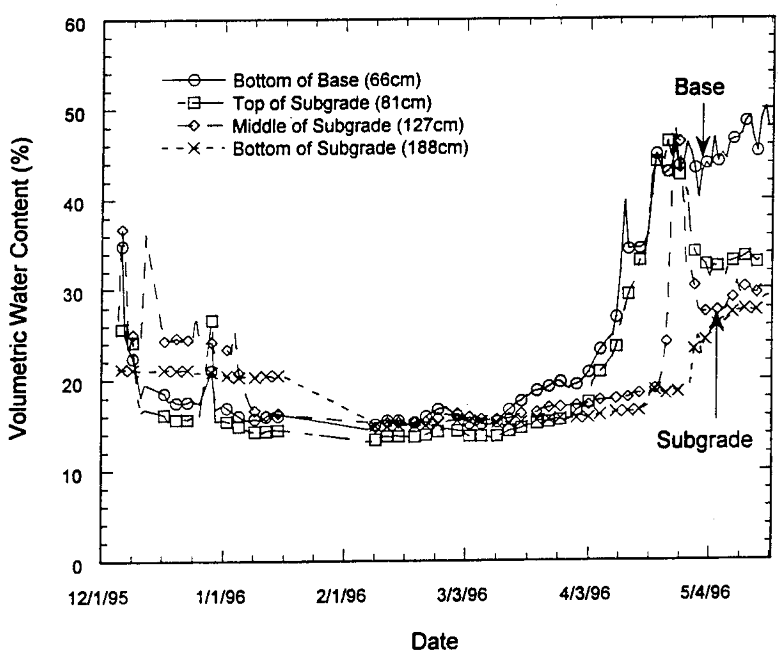

Fig. 4.8. Volumetric water contents at Spirit.

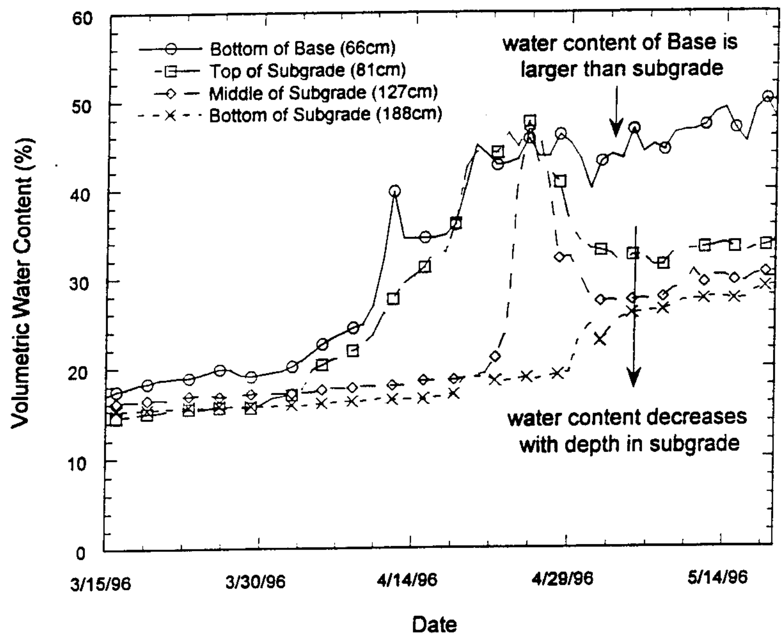

Fig. 4.9. Volumetric water contents during post-thaw period at Spirit.

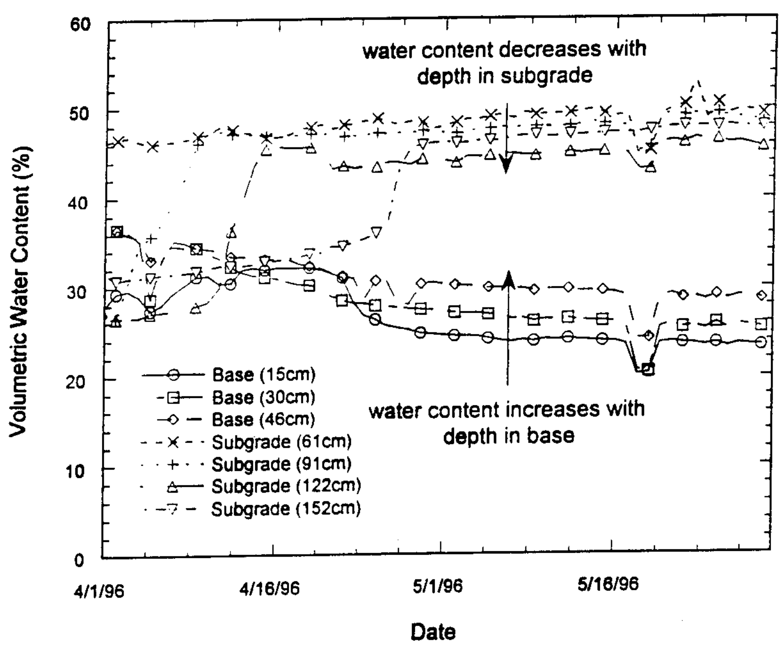

Fig. 4.10. Volumetric water contents during post-thaw period at Westby.

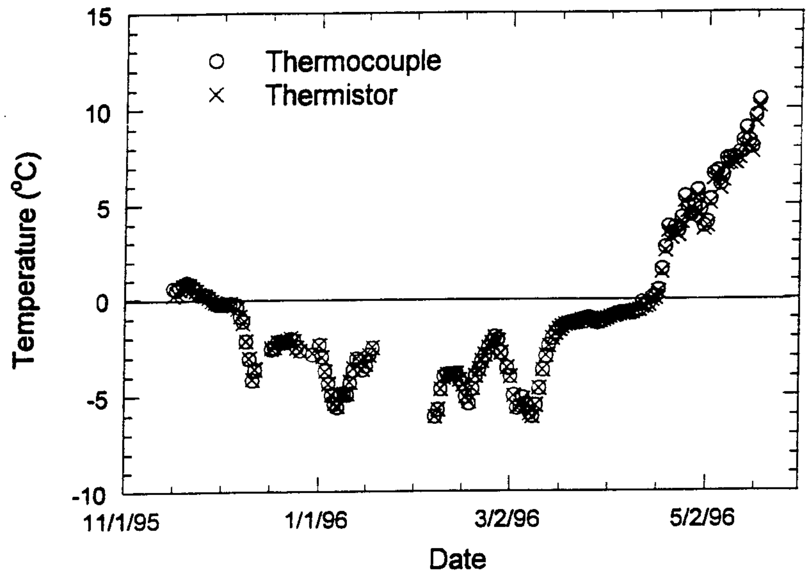

Fig. 4.11. Soil temperatures at depth of 66 cm at Spirit as measured with thermocouples and thermistors.

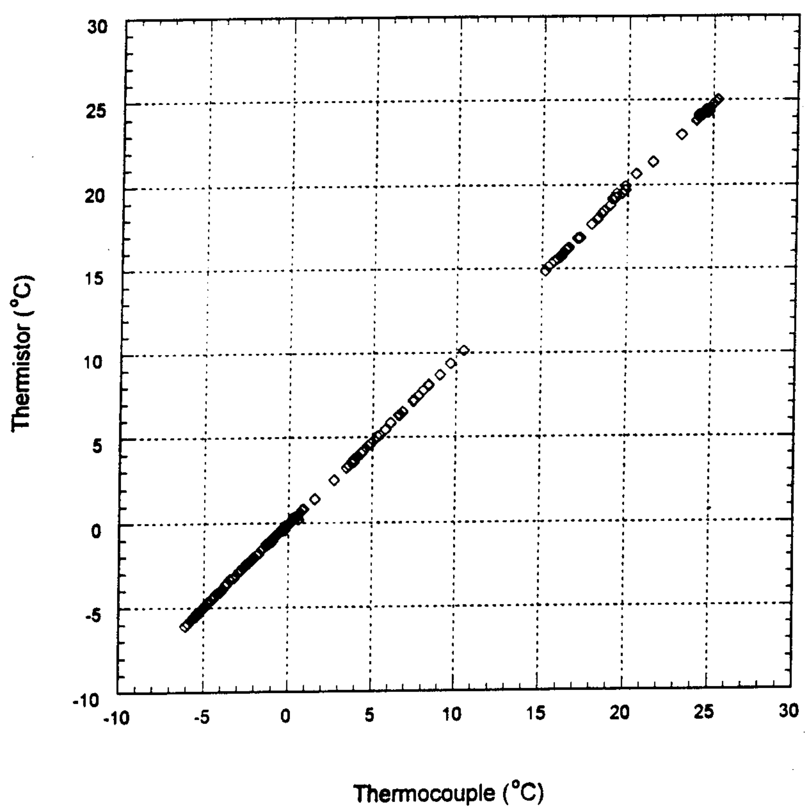

Fig. 4.12. Soil temperatures measured with thermistors vs. temperatures measured with thermocouples: depth = 66 cm, Spirit.

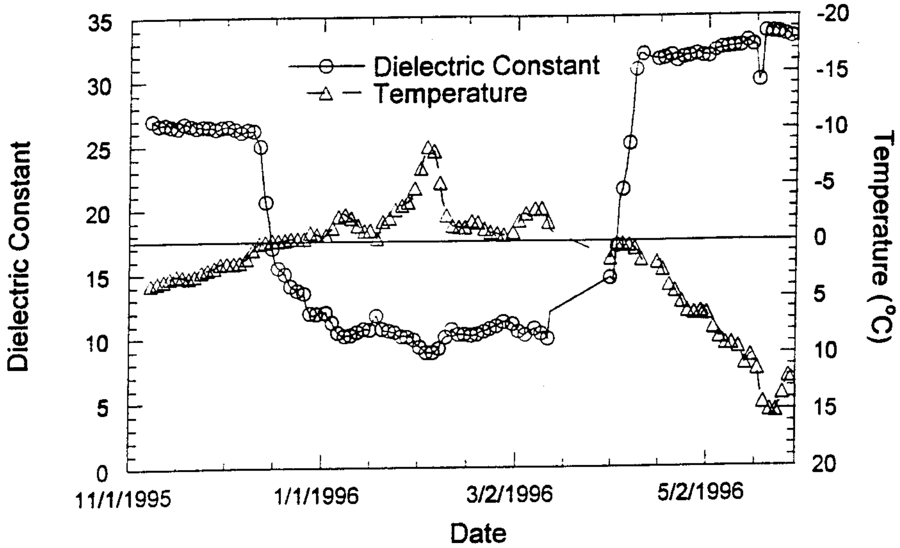

(a)

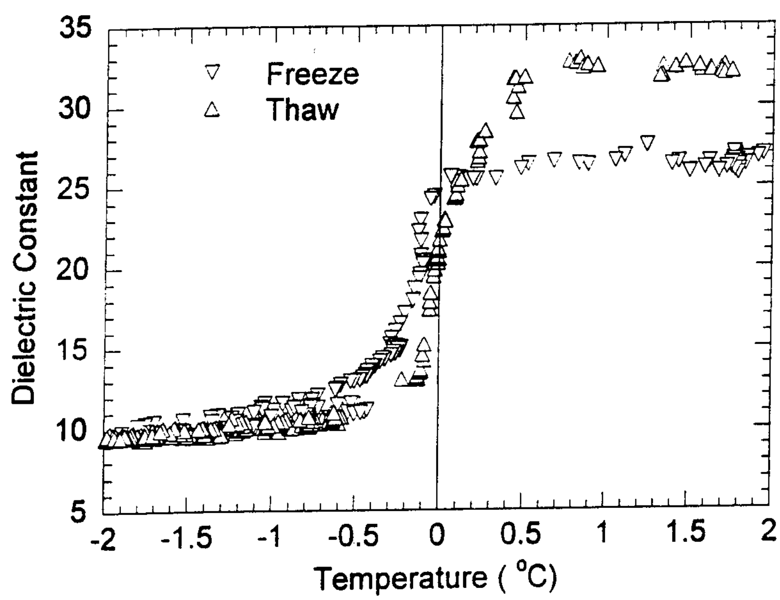

(b)

Fig. 4.13. Dielectric constant and temperature at Westby: (a) Daily average values during 1995-1996, (b) Dielectric constant vs. temperature during freeze and thaw periods (depth = 91 cm).

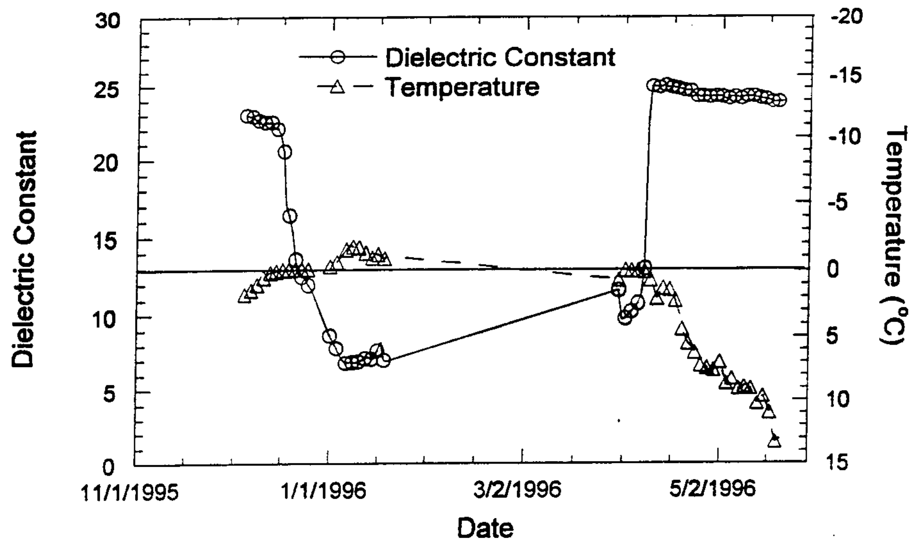

(a)

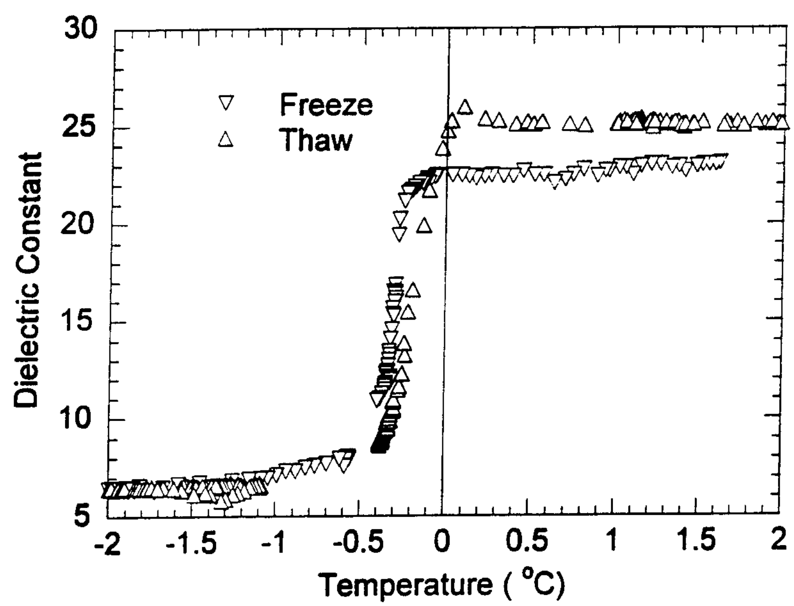

(b)

Fig. 4.14. Soil dielectric constant and temperature at Unity: (a) daily average values during 1995-1996, (b) dielectric constant vs. temperature during freeze and thaw periods (depth = 76 cm).

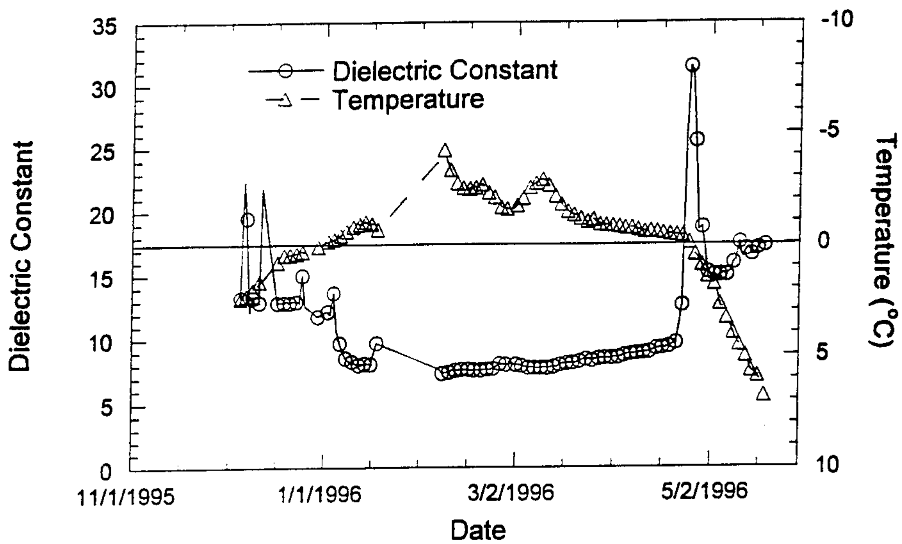

(a)

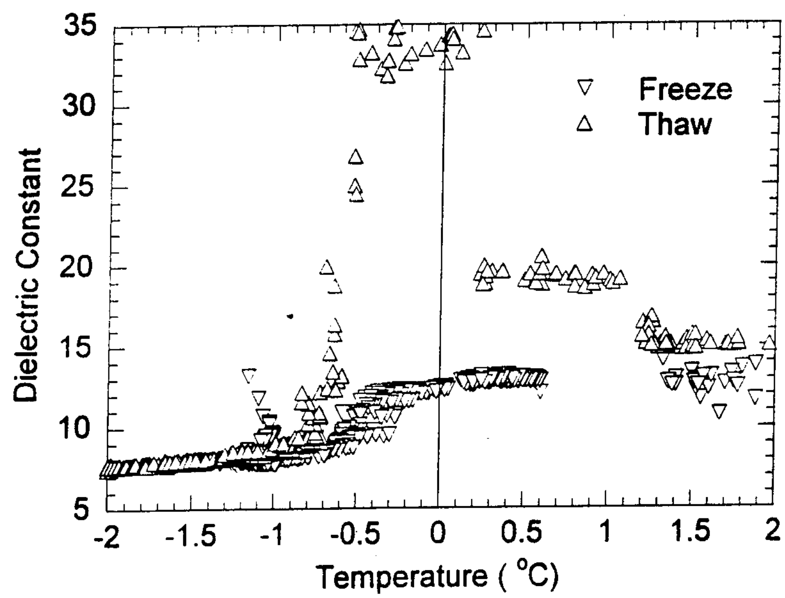

(b)

Fig. 4.15. Dielectric constant and temperature at Spirit: (a) Daily average values during 1995-1996, (b) Dielectric constant vs. temperature during freeze and thaw periods (depth = 127).

Similar phase change temperatures for base and subgrade are reported McBane and Hanek (1986) based on laboratory tests.

4.2.3 Determination of Frost Depth

Frost depths were determined for each pavement structure using the dielectric constant and the phase-change temperature described in Sec. 4.2.2. Frost depths and thaw depths for the Westby and Unity sites are shown in Fig. 4.16 for the 1996-97 monitoring period. The start and end times for freezing and thawing are summarized in Tables 4.1 and 4.2. As Fig. 4.16 shows, the frost and thaw depths obtained using the dielectric constant and temperature data from the thermistors and thermocouples are nearly identical. This suggests that the phase change temperatures are correct.

Freezing of the base course typically begins in mid-November, and the base course is completely frozen by the end of November or the beginning of December (Fig. 4.16). The maximum frost depth is about 1.5 to 1.8 m, with greater frost depth occuring in more northern regions (i.e., Spirit). Thawing begins in mid-March to early April following the classic top-down and bottom-up process. Thawing is complete by the end of April.

4.3 PAVEMENT STIFFNESS

Pavement stiffness was assessed by testing with the FWD from December 1995 through May 1997. Testing occurred approximately each week during the spring thaw period to capture the large and rapid changes in pavement moduli caused by thawing. Frequent testing was also planned for early winter to define changes in modulus caused by freezing of the base and subgrade. However, scheduled maintenance for the FWD and difficulties obtaining accurate measurement in cold air temperatures (< -5 °C) limited testing during the freezing period. Nevertheless, testing was conducted during frozen conditions. During the remainder of the year (May-October), testing was conducted approximately each month provided the FWD was available.

At each site, FWD testing was conducted at stations 15 m apart along a test section centered on the instrumentation trench. Four different load levels (22, 40, 62, and 80 kN) were applied to the pavement surface. Three replicate tests were conducted at each station at each load level. A 22 kN seating drop was also applied at each station before data collection began.

4.3.1 Deflections

Deflection basins measured at Westby are shown in Fig. 4.18. Similar behavior was obtained at the other sites. The basin becomes deeper during the spring when thawing occurs, and then becomes shallower as the pavement recovers during late spring and summer. The deflection basin in fall is similar to that in summer. When the base freezes in early winter, the basin becomes very shallow.

These changes in the deflection basin are caused by changes in the stiffness of the base and subgrade. During thawing, the base and subgrade become soft and thus deeper basins form. In contrast, freezing results in a very stiff base and subgrade, and thus a very shallow basin forms. Summer and fall conditions exist somewhere between these soft and stiff states, and thus a moderately sized deflection basin is obtained in the summer months.

Spatial variation of the maximum deflection is shown in Fig. 4.19 for the 210-m test section at Westby. These deflections were obtained from the 22 kN load. The deflections do not vary spatially for most of the year. But, during the spring thaw, a distinct region exists where the deflection is higher and the pavement system is softer.

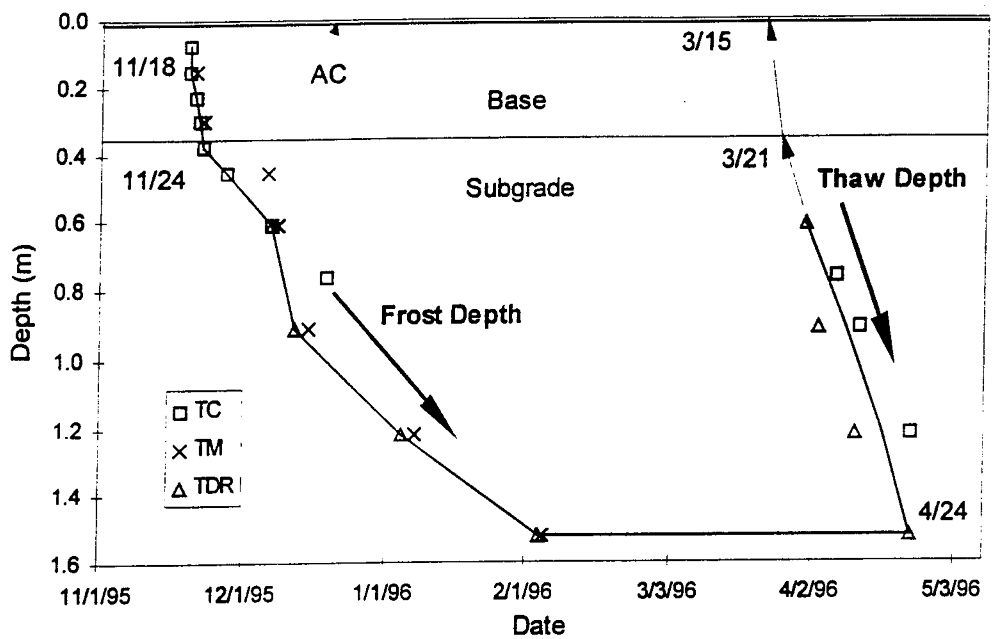

(a)

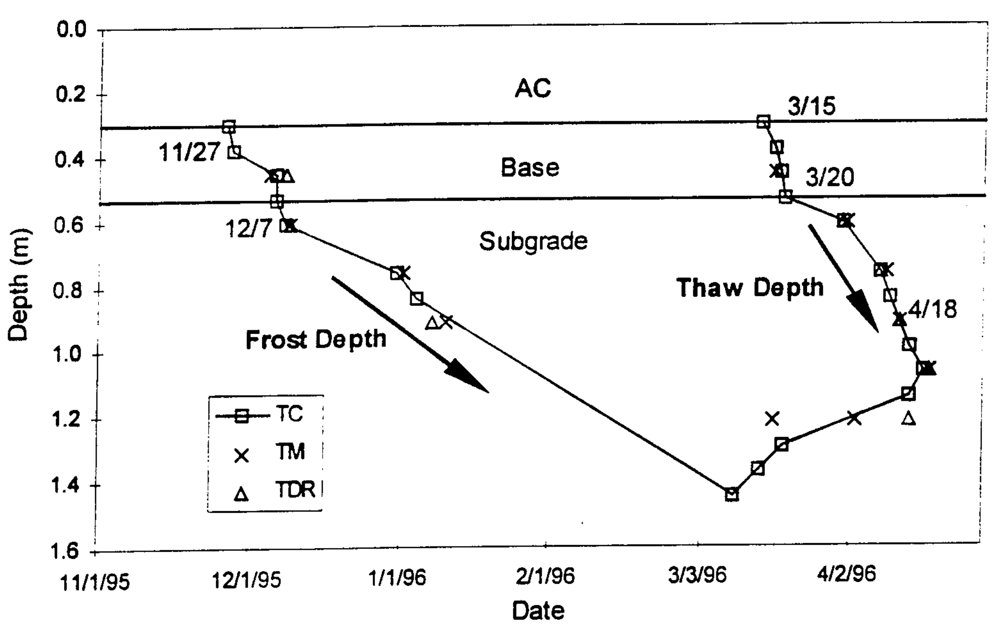

(b)

Fig. 4.16. Freeze and thaw depths at Westby (a) and Unity (b)

Table 4.1. Timing of freezing and thawing for 95-96 monitoring season.

Westby	Frozen		Thaw	
	Begin	End	Begin	End
Base	11/18/95*	11/24/95	3/15/1996*	3/21/96
Subgrade	11/24/95	--	3/21/96	4/24/96

Unity	Frozen		Thaw	
	Begin	End	Begin	End
AC	N/A	11/27/95	N/A	3/15/96
Base	11/27/95	12/7/95	3/15/96	3/20/96
Subgrade	12/7/95	--	3/20/96	4/18/96

Spirit	Frozen		Thaw	
	Begin	End	Begin	End
AC	N/A	11/9/95	N/A	4/1/96
Base	11/9/95	12/5/95	4/1/96	4/16/96
Subgrade	12/5/95	--	4/16/96	4/22/96

*Estimated

Table 4.2. Timing of freezing and thawing for 96-97 monitoring season.

Westby	Frozen		Thaw	
	Begin	End	Begin	End
Base	11/18/96*	11/24/96	3/15/1997*	3/21/97
Subgrade	11/24/96	--	3/21/97	4/24/97

Unity	Frozen		Thaw	
	Begin	End	Begin	End
AC	N/A	11/27/96	N/A	3/15/97
Base	11/27/96	12/7/96	3/15/97	3/20/97
Subgrade	12/7/96	--	3/20/97	4/18/97

Spirit	Frozen		Thaw	
	Begin	End	Begin	End
AC	N/A	11/9/96	N/A	4/1/97
Base	11/9/96	12/5/96	4/1/97	4/16/97
Subgrade	12/5/96	--	4/16/97	4/22/97

*Estimated

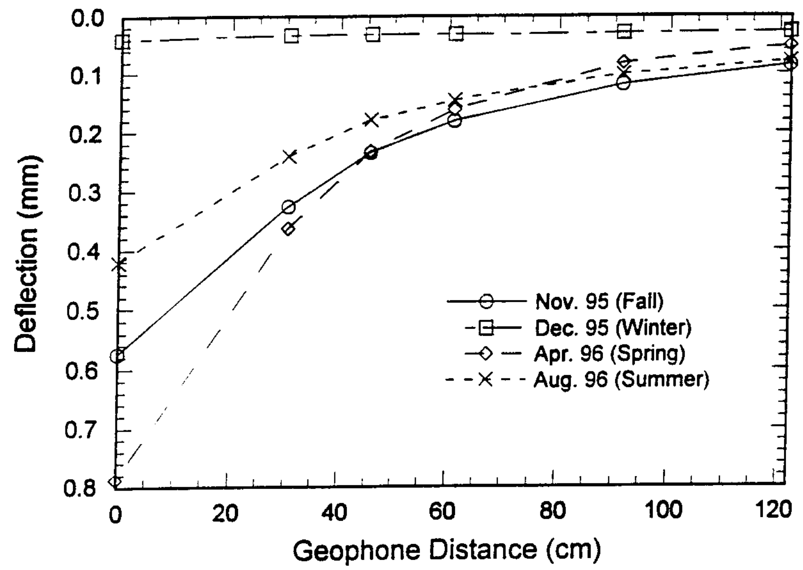

Fig. 4.18. Deflection basins for each season: Westby.

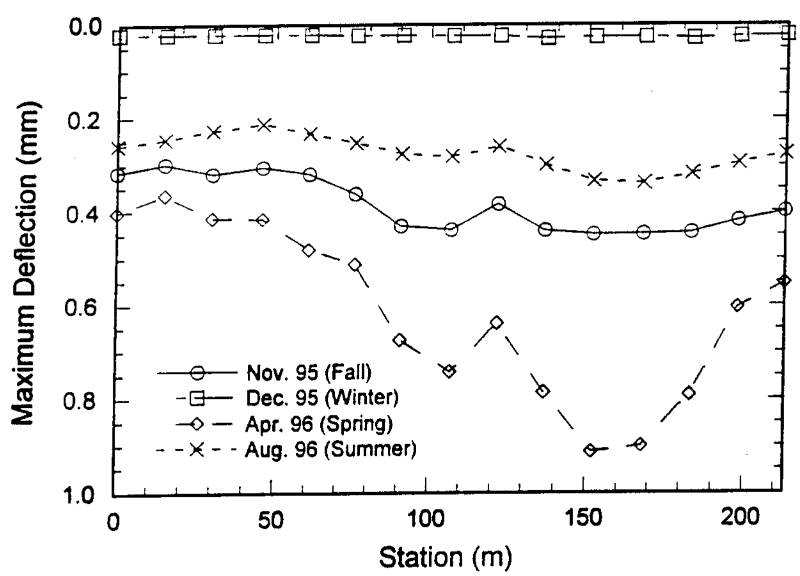

Fig. 4.19. Maximum deflections along Westby test section for each season.

This suggests that a pavement section that appears uniform in summer and fall can become very non-uniform during the spring thaw period.

Deflections along the test section at Spirit are shown in Fig. 4.20 A range of responses was obtained over the 170-m test section. Throughout most of the year (winter excluded), deflections at stations west of the instrumentation trench (≤ 75 m) are smaller than deflections east of the trench (≥ 90 m). This occurred because the AC layer was substantially thicker west of the trench.

4.3.2 Seasonal Variation of Pavement Moduli

The average modulus of the base course and subgrade at Westby are shown in Fig. 4.21a. The modulus of the AC at Westby is not reported, because the layer was very thin and therefore not amenable to analysis, as described in Sec. 3.3.2. The moduli increase dramatically in December due to freezing of the base and subgrade. Then, when thawing begins in late March, the moduli drop dramatically to values below the pre-freezing (i.e., fall) condition. The decrease in modulus is slightly greater for the base. Soon after the moduli reach a minimum, which corresponds to the end of thaw, they begin to slowly increase as a result of drainage. The base recovers more quickly than the subgrade, but full recovery of both layers does not occur until summer.

Similar results were obtained at Unity and Spirit (Fig. 4.21 a,b). At Unity, however, the modulus of the base course underwent greater changes than occurred at Westby or Spirit. Moreover, the modulus of the base course at Spirit was not much different from that of the subgrade, except when frozen. This is likely the result of the poor quality base course at Spirit.

At Unity and Spirit, the modulus of the AC layer was also determined. The changes in modulus of the AC layer correspond well with the seasonal changes in air temperature and solar radiation. However, the AC moduli are generally lower than those predicted with the Asphalt Institute equation (Jong 1997), except when subfreezing conditions exist (December - March). One reason why the AC moduli are lower than moduli predicted with the Asphalt Institute equation is that the AC layers at both sites consist of several overlays that were weakly bonded. A set of weakly bonded layers will have lower effective modulus than a single layer of AC having the same thickness, which is assumed when applying the Asphalt Institute equation.

Typical moduli of each pavement layer corresponding to late-summer conditions are summarized in Table 4.3. The moduli for the AC layers at Unity and Spirit are typical of moduli for AC and the subgrade moduli at all three sites are within typical ranges for fine-grained soils (Lee et al. 1995, Drumm et al. 1990). The moduli of the base courses are more variable. However, they are consistent, at least qualitatively, with conditions observed during installation of the instrumentation. For example, the base course at Westby consisted of high quality crushed gravel, whereas the base course at Spirit was silty sand with a small amount of gravel. Spirit also had the thickest AC layer (34 cm), and this layer consisted of several layers of AC overlays. A softer base course could be responsible for the need to frequently maintain the pavement by adding overlays. In addition, the base course at Unity appeared to be lower in quality than the base at Westby, but better than the base course at Spirit.

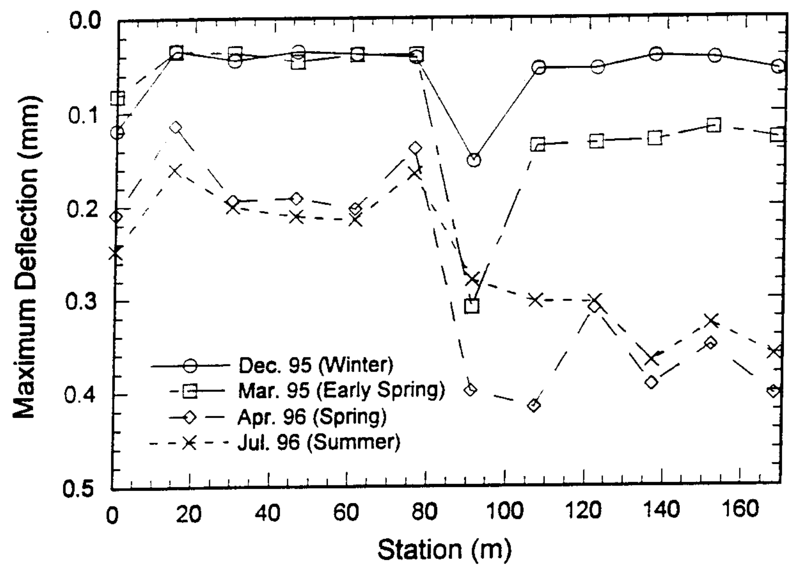

Fig. 4.20. Maximum deflections along test section at Spirit for each season.

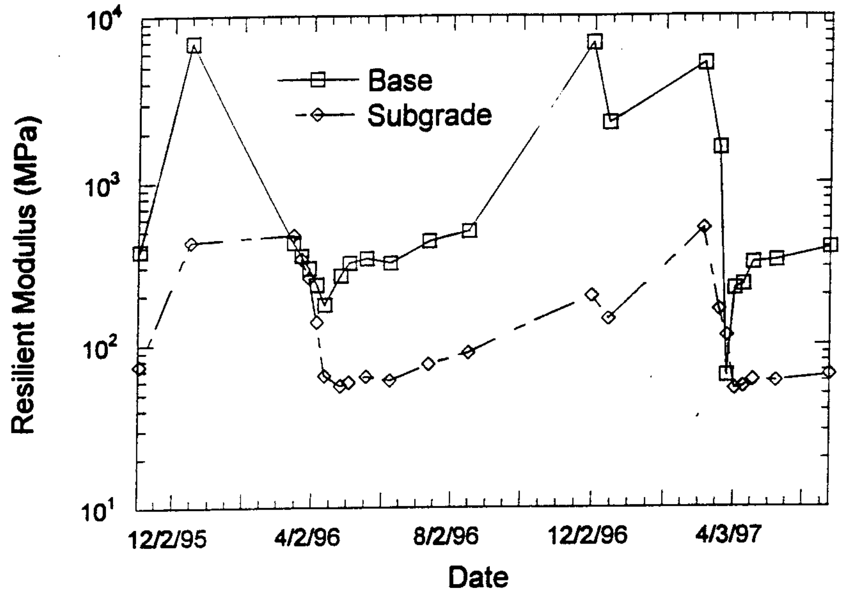

(a)

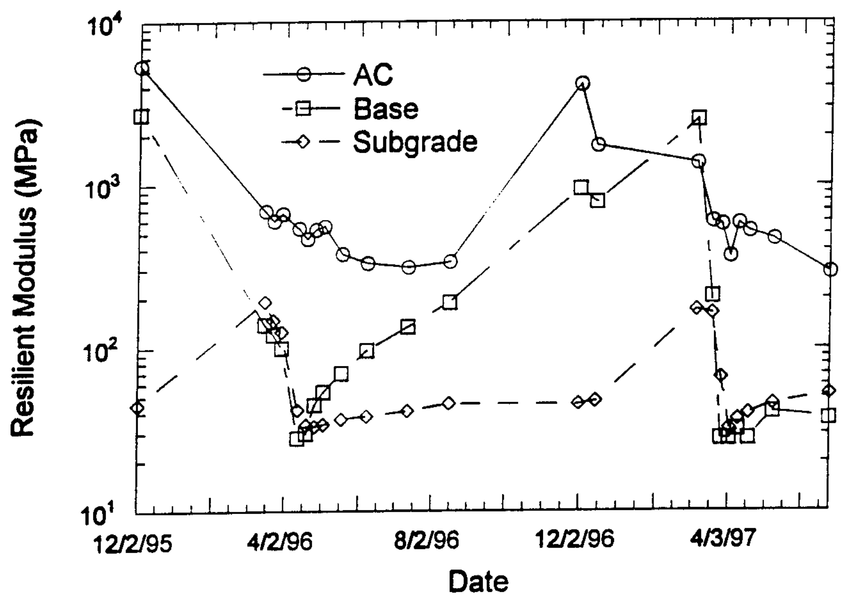

(b)

Fig. 4.21. Moduli of pavement layers: (a) Westby and (b) Unity.

Table 4.3 Late-summer pavement moduli.

Layer	Resilient Modulus (MPa)		
	Westby	Unity	Spirit
Asphalt concrete	N/A	333	674
Base course	500	188	65
Subgrade	89	65	42

4.3.3 Modulus Ratio

Moduli of the pavement layers can be normalized by dividing the modulus at any time by a "typical" modulus corresponding to conditions in late summer or early fall. These normalized moduli are referred to in this report as the modulus ratio. The modulus ratio provides a direct measure of the changes in modulus that occur during freezing, thawing, and post-thawing recovery. Modulus ratios for the Westby, Unity, and Spirit sites are shown in Figs. 5.8 - 5.10. These modulus ratios were normalized using the modulus measured in August. A summary of modulus ratios corresponding to frozen and fully thawed conditions is in Table 4.4.

Table 4.4. Modulus ratios for Westby, Unity and Spirit.

Pavement Layer	Site		
	Westby	Unity	Spirit
Base, frozen	13.8	13.8	15.3
Base, thawed	0.35	0.15	0.47
Subgrade, frozen	5.33	4.23	6.35
Subgrade, thawed	0.63	0.72	0.61

Large changes in modulus of the base course occur at each site when the pavement freezes and thaws. In particular, frozen base course is about 14 to 15 times stiffer than typical base course. At the end of thaw, the modulus of the base course is approximately 15 - 50% of the typical modulus. These large decreases in the modulus of base course are similar to those reported by Mahoney et al. (1985) and Janoo and Berg (1991).

Freezing of the subgrade results in resilient moduli 4 to 6 times the typical moduli. Conversely, thawing results in a reduction in modulus that ultimately is 60 - 70% of the typical modulus. This reduction in modulus is similar to the 40% reduction in modulus reported by Lee et al. (1995) and the 23% reduction in modulus reported by Mahoney et al. (1985)

Examination of Fig. 4.22 shows that the temporal changes in modulus ratio for the base and subgrade are similar at each site. Thus, a general relationship can be developed that describes temporal changes in modulus ratio. This relationship was identified by analyzing the data for the freezing, thawing, and recovery periods separately. These periods are shown in Fig. 4.22 for each site. Because the time during which thawing and recovery occur are different at each site, time was normalized by defining the time ratio, T:

$$T = \frac{t - t_b}{t_e - t_b} \tag{4.1}$$

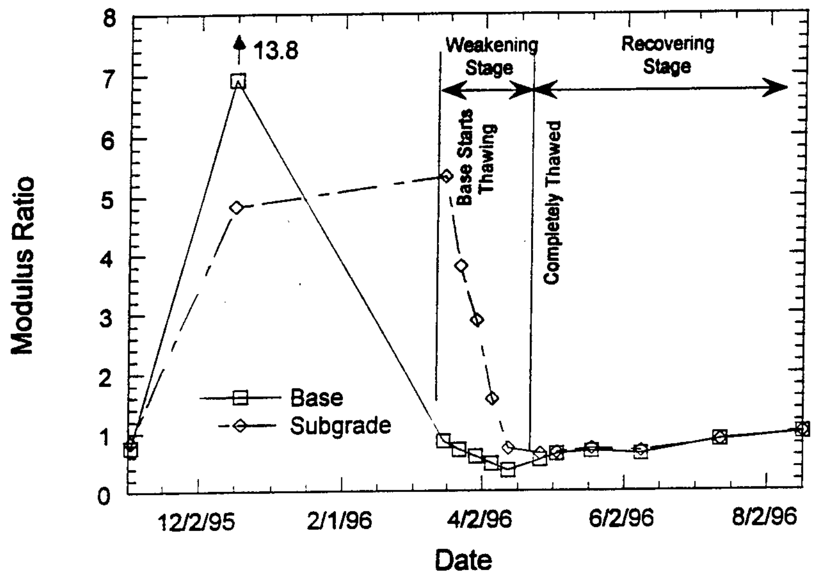

(a)

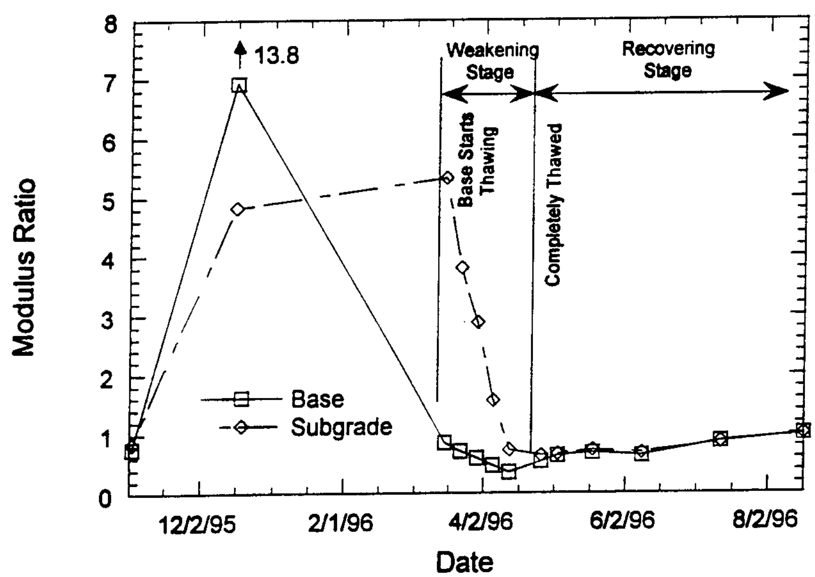

(b)

Fig. 4.22. Modulus ratio as a function of time: (a) Westby and (b) Unity.

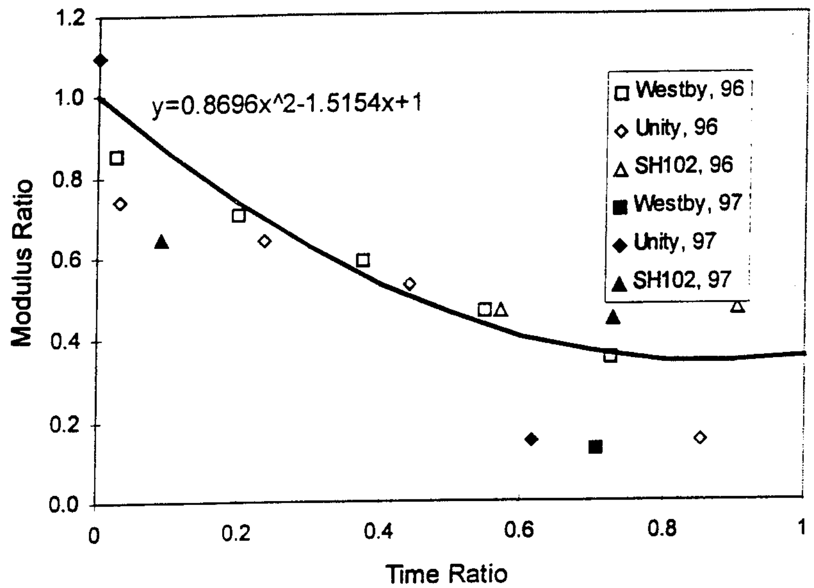

(a)

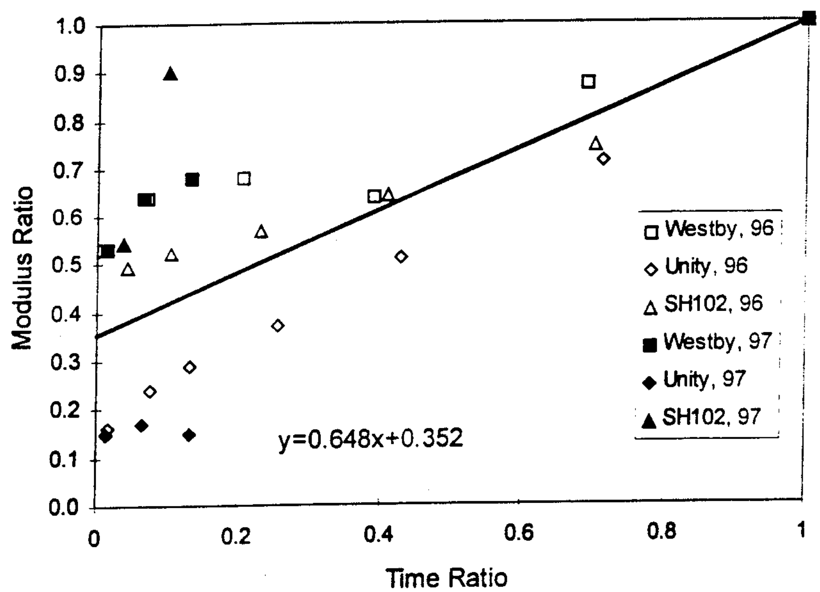

(b)

Fig. 4.23. Modulus ratio vs. time ratio for base course: (a) thawing and (b) recovery.

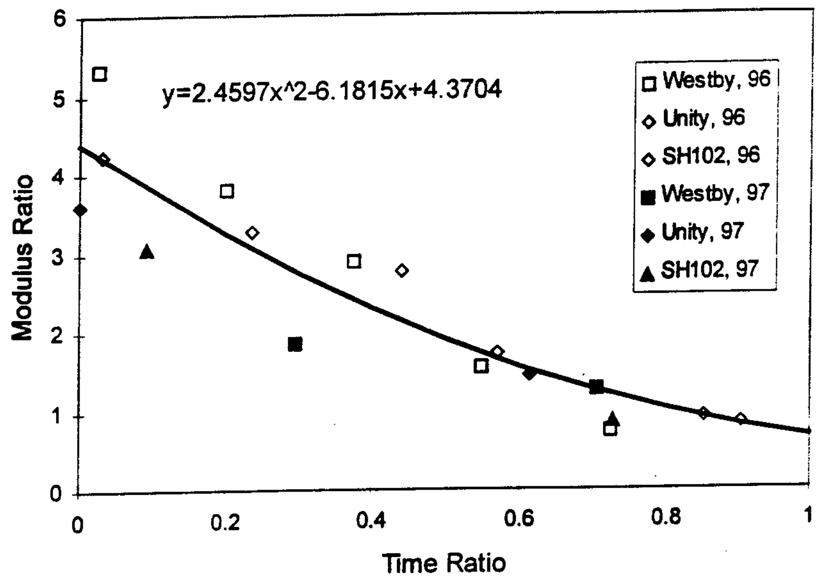

(a)

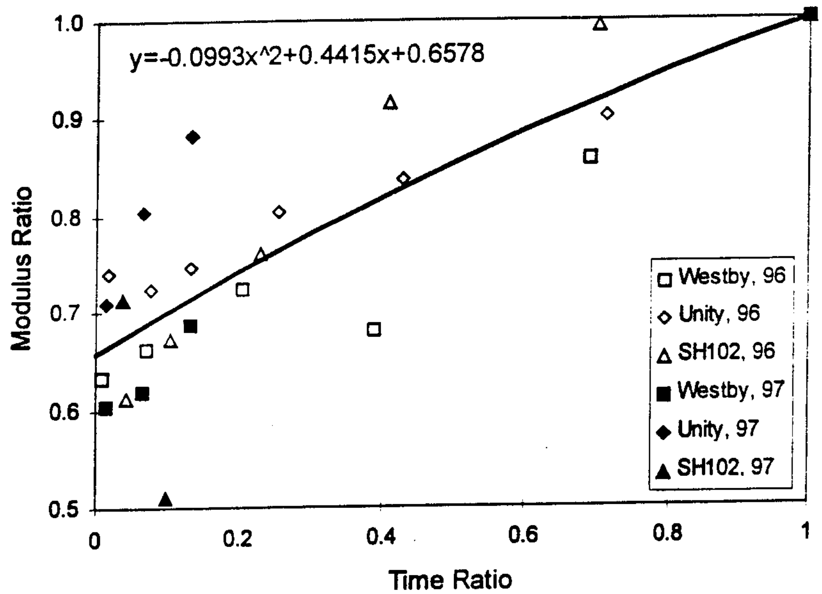

(b)

Fig. 4.24. Modulus ratio vs. time ratio for subgrade: (a) thawing and (b) recovery.

where t is time, t_b is the time at which a particular period begins, and t_e is the time at which a period ends. For thawing, t_b is the beginning of thaw and t_e is the end of thaw. Similarly, for recovery t_b is the beginning of recovery, and t_e is the end of recovery. Because recovery begins at the end of thaw, t_b for recovery equals t_e for thaw. The end of recovery was assumed to be August 1 for all sites.

Modulus ratio vs. time ratio for thawing and recovery is shown in Fig. 4.23 for the base course and Fig. 4.24 for the subgrade. The data fall within a reasonably narrow band for thawing and recovery and the band is similar for the data collected in 1996 and 1997. Second-order polynomials were fit to the bands of data using least squares regression (solid lines in Figs. 4.23 and 4.24). These functions have the form:

$$R_m = \alpha T^2 + \beta T + \delta \tag{4.2}$$

where R_m is the modulus ratio. Table 4.4 is a summary of the regression coefficients α, β, and δ in Eq. 4.3.

Table 4.3. Regression coefficients for Eq. 4.2.

Layer & Condition	α	β	δ
Base Thawing	0.87	-1.52	1.00
Base Recovery	0	0.65	0.35
Subgrade Thawing	2.46	-6.18	4.37
Subgrade Recovery	-0.09	0.44	0.66

A comparison of the measured moduli and moduli predicted using Eq. 4.2 is shown in Fig. 4.25. The predicted and measured moduli are in good agreement.

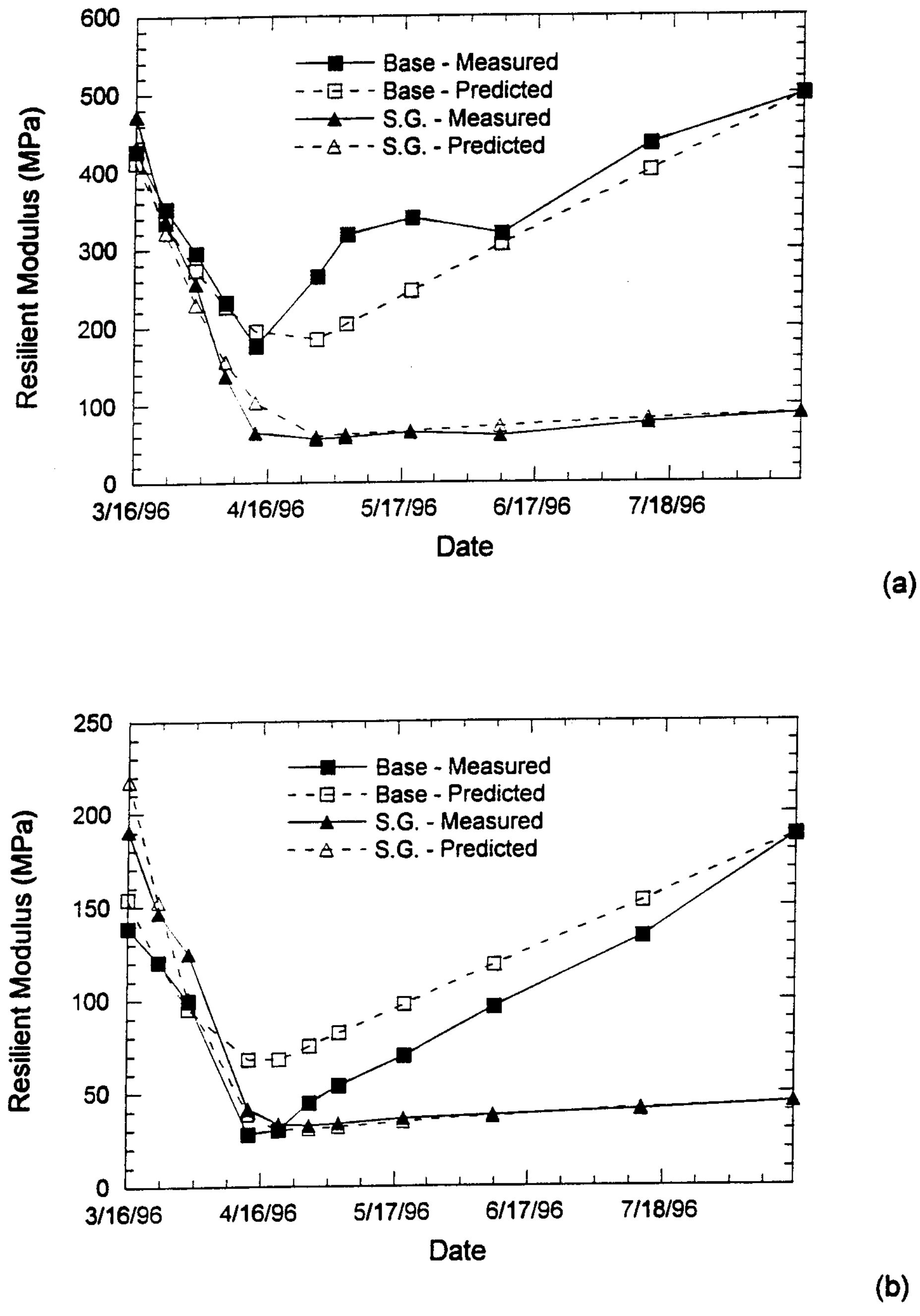

Fig. 4.25. Moduli measured and predicted using Eq. 4.2: (a) Westby and (b) Unity.

SECTION 5
SUMMARY AND CONCLUSIONS

The objective of this study was to develop a method that the Wisconsin Dept. of Transportation can use to predict the timing for permissible overload declarations when flexible pavements freeze and weight restrictions when flexible pavements thaw. To meet this objective, three sections of secondary highways with flexible pavements were instrumented and monitored to determine how freezing, thawing, and post-thaw recovery affect pavement stiffness. Two sites (Unity and Spirit) were located in northern Wisconsin, whereas the other site (Westby) was located in western Wisconsin. Data collected from these sites were used to develop a computer model (UWFrost) that can be used to predict seasonal changes in pavement capacity. The computer model is described in a separate document (Bosscher et al. 1998).

Freezing and thawing were found to have a significant effect on the stiffness and capacity of flexible pavements. The pavement stiffens during winter when the base freezes, and softens substantially when the base and subgrade thaw. The softening (or decrease in modulus) occurs rapidly after the onset of thawing. A gradual recovery process occurs after thawing is complete. This recovery process, during which the pavement stiffens, continues until mid-summer. The base undergoes the largest changes in modulus during freezing and thawing, and also recovers quicker. In contrast, the subgrade recovers slowly during the post-thaw recovery period. The changes in modulus in the base and subgrade can be characterized by a non-dimensional modulus ratio, which is normalized to the modulus existing in late summer. The computer model described in Bosscher et al. (1998) incorporates functions describing how the modulus ratio changes during freezing, thawing, and recovery.

The computer model can be used to simulate how freezing and thawing affect the stiffness and capacity of pavements. The user inputs meteorological data for the pavement location, defines the pavement location on the Wisconsin map, defines the pavement layer geometry, and enters criteria regarding the historical data to be used and the prediction period that is desired. These data are then used in a one-dimensional heat transfer model that simulates geothermal conditions and defines the depths of freezing and thawing. The heat transfer model uses historical meteorological data when predicting subsurface conditions in the future.

The depths of freezing and thawing are used to define the modulus of each pavement layer through the modulus ratio functions obtained from the field experiments. The pavement moduli are then used in a layered elastic analysis to determine stresses and strains in the pavement layers. The elastic analysis is conducted iteratively using different loads until the load is found that induces no more damage than a design load applied during late summer. This load is referred to as the equivalent damage load (EDL). EDLs are defined for fatigue and rutting damage.

The computer model predicts EDLs for each day during the prediction period selected by the user. EDLs are as much as three times higher than design loads when the base and subgrade are frozen. This suggests that significant overloads can be permitted without incurring excessive damage when a flexible pavement is frozen. At the end of thaw, when the pavement reaches its softest condition, the EDL can be less than one-half the design load. Thus, weight restrictions less than 50% of the design load may be necessary to prevent damage during the thawing period.

SECTION 6
RECOMMENDATIONS

The computer model developed in this study (UWFrost, Bosscher et al. 1998) has been written based on field observations made over a two-year period (1995-1997). These two years had average winters. Thus, predictions made with the computer model should represent average responses of pavements subjected to freezing and thawing. However, conditions existing during particularly severe or mild winters may not be accurately represented by the model. To accurately describe these extreme conditions, more data should be collected and used to check the model.

Full validation of the model will also require that data be collected on maintenance costs for pavements where the model has been used to establish load limits and on pavements where the model has not been used. An evaluation program should begin as soon as the model is implemented to determine if benefits are being derived from its use.

To obtain the best long-term performance from the model, a monitoring program should be implemented that measures pavement performance (via Falling Weight Deflectometer, Spectral Analysis of Surface Waves, or similar equipment) as a function of time for many additional sites. Additional data are needed to make the model more accurate. This is especially critical during the spring thaw. The model has been flexibly written such that future updates to key coefficients such as the thawing and recovery regression parameters can be easily made based on this additional data. Accordingly, the model should be regularly evaluated and updated as additional data and experience become available.

SECTION 7
REFERENCES

AASHTO (1993), *"AASHTO Guide for Design of Pavement Structures,"* American Association of State Highway and Transportation Officials, Washington, D.C.

Andersland, O. and Ladanyi, B. (1994), *An Introduction to Frozen Ground Engineering,* Chapman & Hall, New York.

Asphalt Institute (1982), *Research and Development of the Asphalt Institute's Thickness Design, Manual (MS-1), Research Report No. 82-2*, Ninth Edition, Asphalt Institute, College Park, Maryland.

Asphalt Institute (1991), *Thickness Design-Asphalt Pavements for Highways and Streets*, Manual Series No. 1, Asphalt Institute, College Park, Maryland.

Barcomb, J. (1989), "Use of Thermistors for Spring Road Management," *Transportation Research Record 1252*, Transportation Research Board. National Research Council, Washington, D.C., pp.12-20.

Bentsen, R., Nazarian, S., and Harrison, J. (1989) "Reliability Testing of Seven Nondestructive Pavement Testing Devices," *Nondestructive Testing of Pavements and Backcalculation of Moduli,* STP 1026, ASTM, Philadelphia, Pennsylvania, pp. 41-58.

Bosscher, P., Jong, D., and Benson, C. (1998), User's Guide for UWFrost, Geotechnical Engineering Report 98-11, Dept. of Civil & Environmental Engineering, University of Wisconsin-Madison.

Braley, W. and Zarling, J. (1990), "MUT1D, Multilayer User-Friendly Thermal Model in 1 Dimension," Alaska Dept. of Transportation and Public Facilities, Report No. FHWA-AK-RD-90-02.

Chen, D., Zaman, M., and Laguros, J. (1994), "Assessment of Distress Models for Prediction of Pavement Service Life," *Proc. of the Third Material Engineering Conference*, pp.1073-1080.

Drumm, E., Boateng-Poku, Y., and Pierce, T. (1990), "Estimation of Subgrade Resilient Modulus for Standard Tests," *Journal of Geotechnical Engineering*, ASCE, Vol. 116, No. 5, pp. 774-779.

FHWA (1994), *Pavement Deflection Analysis*, Report No. 13127, National Highway Institute, Federal Highway Administration.

Horak, E. (1987), "The Use of Surface Deflection Basin Measurements in the Mechanistic Analysis of Flexible Pavements," *Proc. Sixth International Conference Structural Design of Asphalt Pavements*, University of Michigan, Ann Arbor.

Janoo, V. and Berg, R. (1990), "Predicting Pavement Response during Thaw Weakening Periods Using the Falling Weight Deflectometer," *Proc. of the Third International Conference, Bearing Capacity of Roads and Airfields.* Vol.2, pp.31-40.

Janoo, V. and Berg, R. (1990), *"Predicting the Behavior of Asphalt Concrete Pavements in Seasonal Frost Areas Using Nondestructive Techniques,"* CRREL Report 90-10, U.S. Army Corps of Engineers, Cold Regions Research and Engineering Laboratory, Hanover, NH.

Janoo, V., and Berg, R. (1991), *"Performance of Asphalt concrete Airport Pavements During Thaw Weakening Periods: A Field Study,"* CRREL Report 91-7, U.S. Army Corps of Engineers, Cold Regions Research and Engineering Laboratory, Hanover, NH.

Janoo, V., and Berg, R. (1996), *"PCC Airfield Pavement Response During Thaw-Weakening Periods: A Field Study,"* CRREL Report 96-12, U.S. Army Corps of Engineers, Cold Regions Research and Engineering Laboratory.

Johnson, T., Cole, D. and Chamberlain, E. (1978), *"Influence of Freezing and Thawing on the Resilient Properties of a Silt Soil Beneath an Asphalt Concrete Pavement,"* Report 78-23, U.S. Army Corps of Engineers, Cold Regions Research and Engineering Laboratory, Hanover, NH.

Johnson, T., Cole, D. and Erwin, L. (1982), "Characterization of Freeze/Thaw-Affected Granular Soils for Pavement Evaluation." *Proc. Fifth International Conference on Structural Design of Asphalt Pavements,* University of Michigan, Ann Arbor, pp. 805-817.

Jong, D. (1997), "Freeze-Thaw Effects on the Stiffness of Flexible Pavement Systems, MS Thesis, Dept. of Civil and Environmental Engineering, University of Wisconsin-Madison.

Lee, W., Bohra, N., Altschaeffl, A., and White, T. (1995), "Resilient Modulus of Cohesive Soils and the Effect of Freeze-Thaw," *Can. Geotech. J.,* Vol.31, pp.559-568.

Leonards, G. and Andersland, O. (1960), "The Clay-Water System and the Shearing Resistance of Clays," *Research Conference on Shear Strength of Cohesive Soils,* ASCE, pp. 793-818.

Mahoney, J., Lary, J., Sharma, J., and Jackson, N. (1985), "Investigation of Seasonal Load Restrictions in Washington State," *Transportation Research Record 1043,* Transportation Research Board, National Research Council, Washington, D.C., pp. 58-67.

Mahoney, J., Rutherford, M., and Hicks, R. (1987), *Guidelines for Spring Highway Use Restriction,* FHWA-TS-87-209, Federal Highway Administration, U.S. Department of Transportation.

Martinelli, T. (1977), *The Use of Frost Depth Indicators in Wisconsin Highways, Summary Report,* Wisconsin Department of Transportation.

McBane, J. and Hanek, G. (1986), "Determination of the Critical Thaw-Weakened Period in Asphalt Pavement Structures," *Transportation Research Record 1089*, Transportation Research Board, National Research Council, Washington, D.C., pp.138-146.

Nordal, R. (1982), "Detection and Prediction of Seasonal Changes of the Bearing Capacity at the Vormsund Test Road," *Proc. International Symposium on Bearing Capacity of Roads and Airfields,* Trondheim, Norway, pp. 374-382.

Nordal, R., and Hansen, E. (1987), *The Vormsund Test Road, Part 4: Summary Report,* Norwegian Road Research Laboratory.

Rada, G., Lopez, A., Elkins, G., Richter, C., and Henderson, B. (1995), "Long-Term Pavement Performance Seasonal Monitoring Program: Instrumentation Selection and Installation," *Transportation Research Record 1432*, Transportation Research Board, National Research Council, Washington, D.C., pp. 32-43.

Rutherford, M., and Mahoney, J. (1986), "A Thermal Analysis of Pavement Thawing," *Proceedings of the Fourth International Conference on Cold Regions Engineering,* ASCE, New York, NY. pp. 369-383.

Rwebangira, T., Rutherford, M., Mahoney, J., and Hicks, R. (1987), "Development of Spring Load restrictions for Local Roads," *Transportation Research Record 1128*, Transportation Research Board, National Research Council, Washington, D.C., pp. 42-52.

Samuelson, M. and Benson, C. (1997), Predicting Frost Depths Beneath Flexible Roadways Using a Thermal Model, Environmental Geotechnics Report 97-5, Dept. of Civil and Environmental Engineering, University of Wisconsin-Madison.

Scrivner, F., Peohl, R., and Phillips, M. (1969), "Detecting Seasonal Changes in Load-Carrying Capabilities of Flexural Pavements," NCHRP Report No. 76, Highway Research Board, Washington, D.C.

Shell (1978), *Shell Pavement Design Manual*, Shell International Petroleum, Co. Ltd.

Smith, M. and Tice, A. (1988), "Measurements of the Unfrozen Water Content of Soils: Comparison of NMR and TDR Methods," Report No. 88-18, U.S. Army Corps of Engineers, Cold Regions Research and Engineering Laboratory, Hanover, NH.

SHRP (1993), *SHRP's Layer Moduli Backcalculation Procedure,* SHRP-P-655, Strategic Highway Research Program, National Research Council, Washington, D.C.

Thomassen, T. and Eirum, R. (1982), "Norwegian Practices for Axle Load Restrictions in Spring Thaw," *Proc. International Symposium on Bearing Capacity of Roads and Airfields,* Trondheim, Norway, pp. 921-930.

Thompson, M. and Robnett, Q. (1979), “Resilient Properties of Subgrade Soils,” *Journal of Transportation Engineering*, ASCE, Vol. 105, No. TE1, pp.71-89.

Topp, G., Davis, J., and Annan, A. (1980), Electromagnetic Determination of Soil Water Content: Measurements in Coaxial Transmission Lines, Water Resources Research, Vol. 16, No. 3, pp. 574-582.

TTI (1991), *MODULUS 4.0, User's Manual,* Texas Transportation Institute, Texas A&M University.

Ullidtz, P. (1987), *Pavement Analysis,* Developments in Civil Engineering, Elsevier.

Uzan, J. (1994), “Advanced Backcalculation Techniques,” *Nondestructive Testing of Pavements and Backcalculation of Moduli,* STP 1198, ASTM, Philadelphia, pp. 3-37.

van Caulwelaert, F., Alexander, D., White, T., and Barker, W. (1989), "Multilayer Elastic Program for Backcalculating Program for Backcalculating Layer Moduli," *Nondestructive Testing of Pavements and Backcalculation of Moduli, STP 1026*, A. Bush and G. Baladi, eds., ASTM, Philadelphia, pp. 171-188.

Yesiller, N., Benson, C., and Bosscher, P. (1995), Comparison of Load Restriction Timings Determined Using FHWA Guidelines and Frost Tubes, *J. of Cold Regions Eng.,* ASCE, 10(1), 6-24.

Appendix
Field Meteorological and Subsurface Data

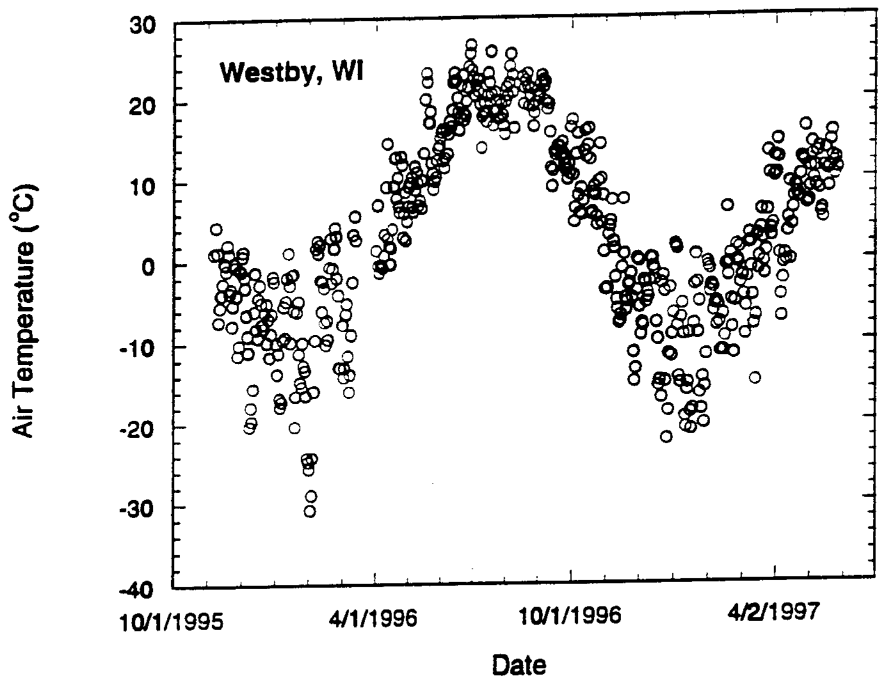

Westby, WI
Air Temperature (°C)
30
20
10
0
-10
-20
-30
-40
10/1/1995
4/1/1996
10/1/1996
4/2/1997
Date

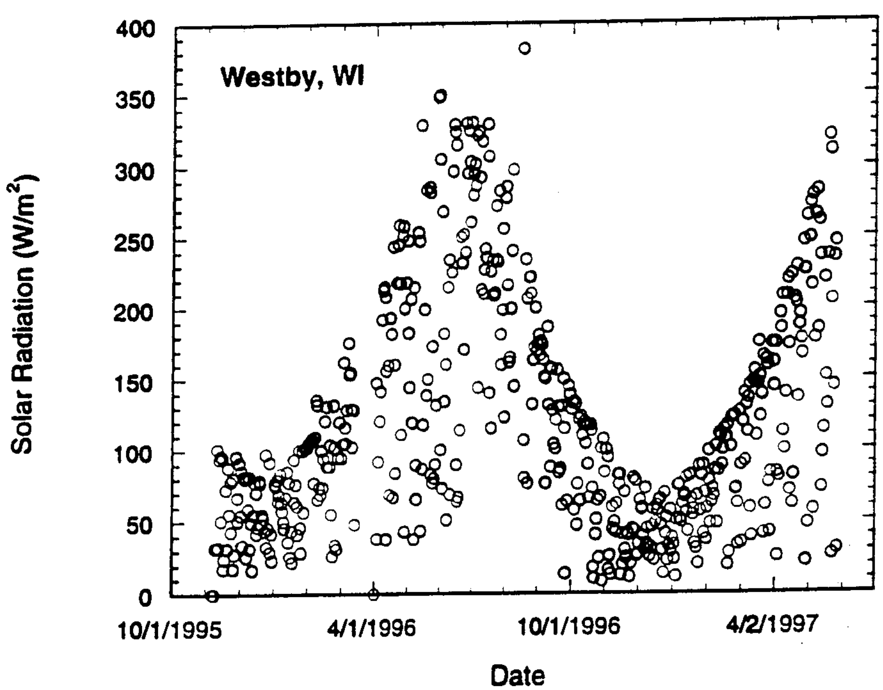

Westby, WI
Solar Radiation (W/m²)
400
350
300
250
200
150
100
50
0
10/1/1995
4/1/1996
10/1/1996
4/2/1997
Date

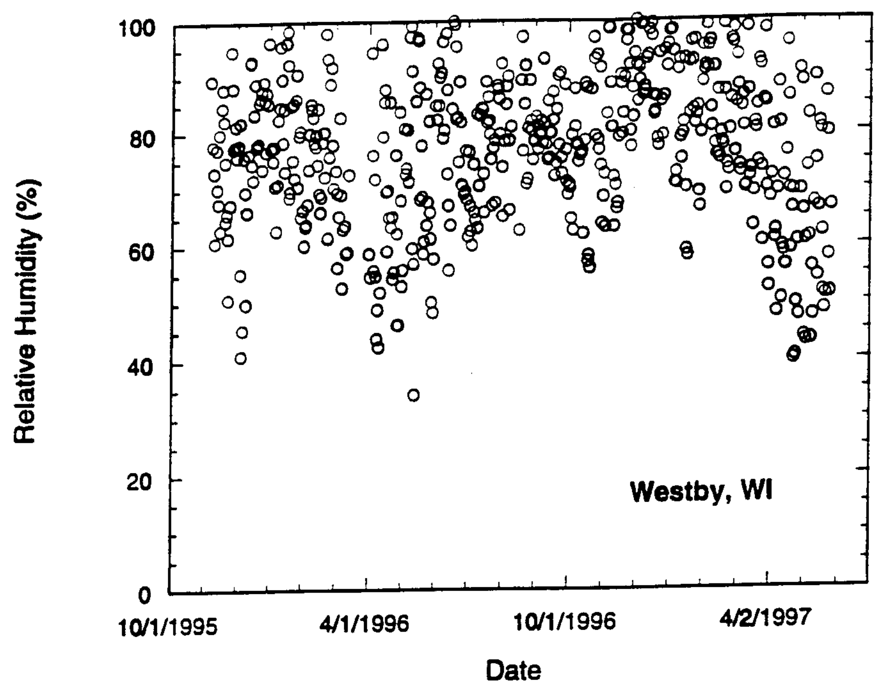

100
80
60
40
20
0
Relative Humidity (%)
Westby, WI
10/1/1995
4/1/1996
10/1/1996
4/2/1997
Date

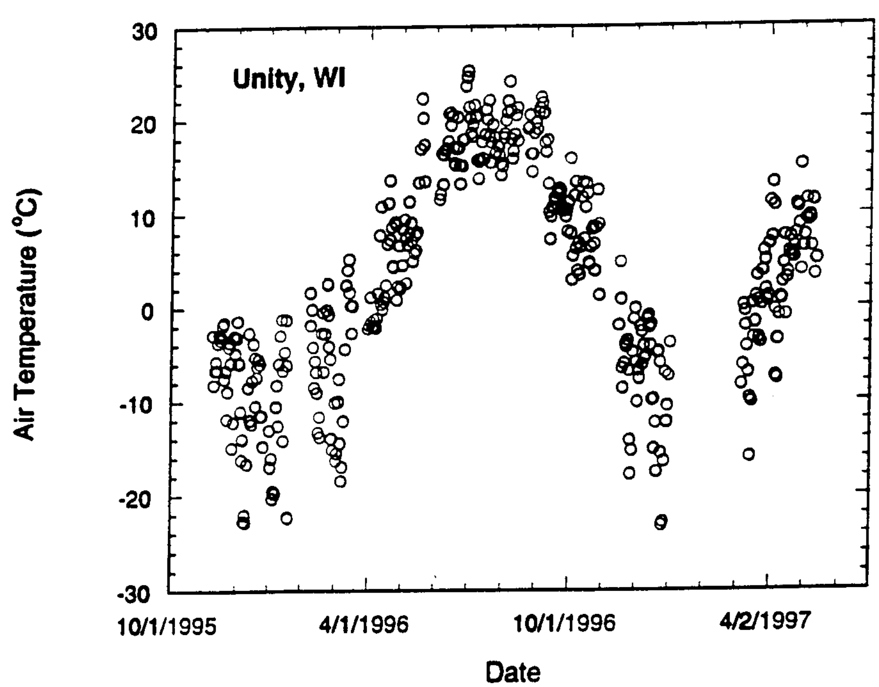

30
20
10
0
-10
-20
-30
Air Temperature (°C)
Unity, WI
10/1/1995
4/1/1996
10/1/1996
4/2/1997
Date

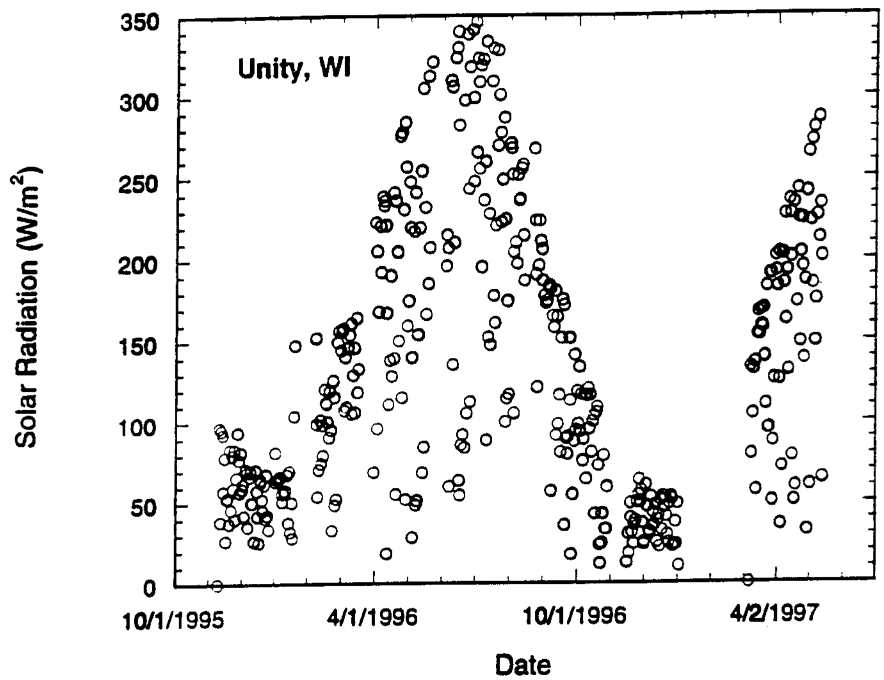
Unity, WI
Solar Radiation (W/m^2)
0
50
100
150
200
250
300
350
10/1/1995
4/1/1996
10/1/1996
4/2/1997
Date

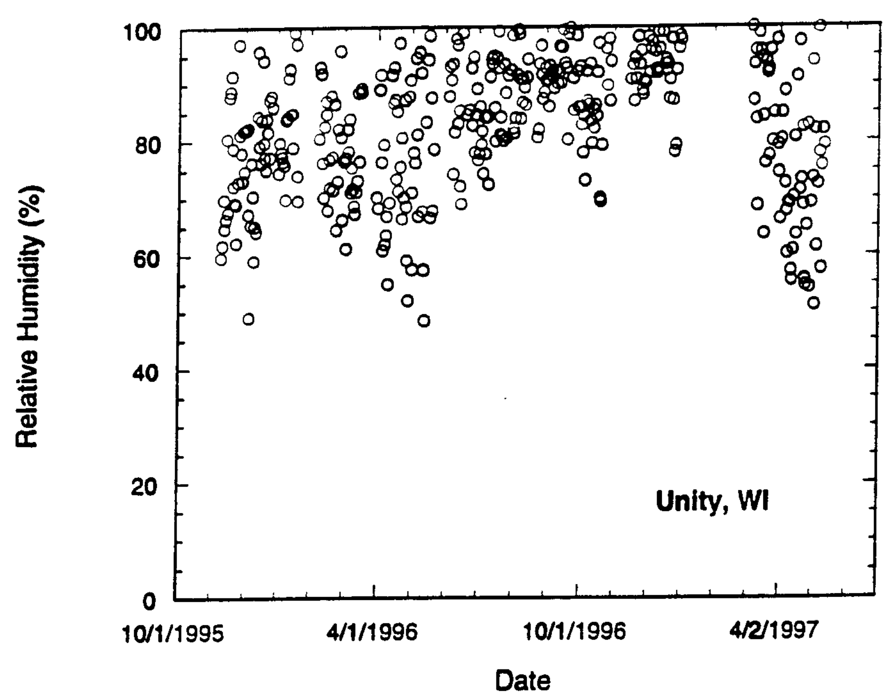
Unity, WI
Relative Humidity (%)
0
20
40
60
80
100
10/1/1995
4/1/1996
10/1/1996
4/2/1997
Date

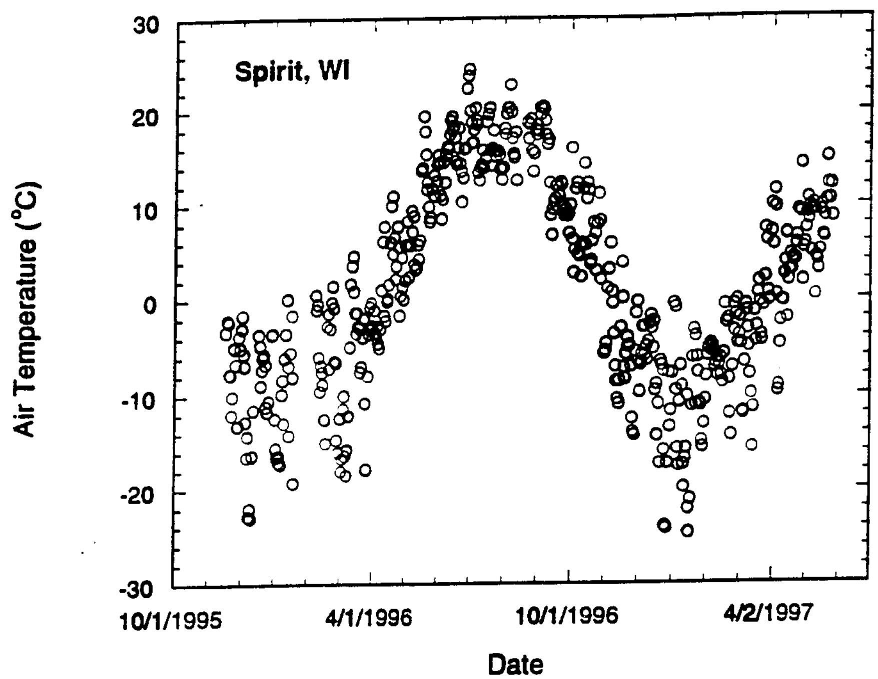
Spirit, WI
Air Temperature (°C)
30
20
10
0
-10
-20
-30
10/1/1995
4/1/1996
10/1/1996
4/2/1997
Date

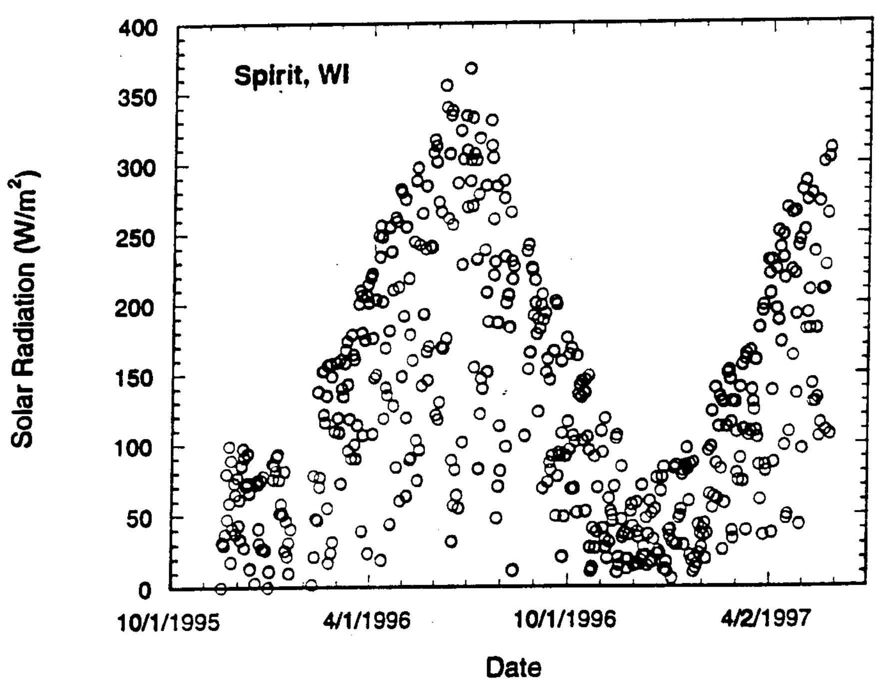
Spirit, WI
Solar Radiation (W/m²)
400
350
300
250
200
150
100
50
0
10/1/1995
4/1/1996
10/1/1996
4/2/1997
Date

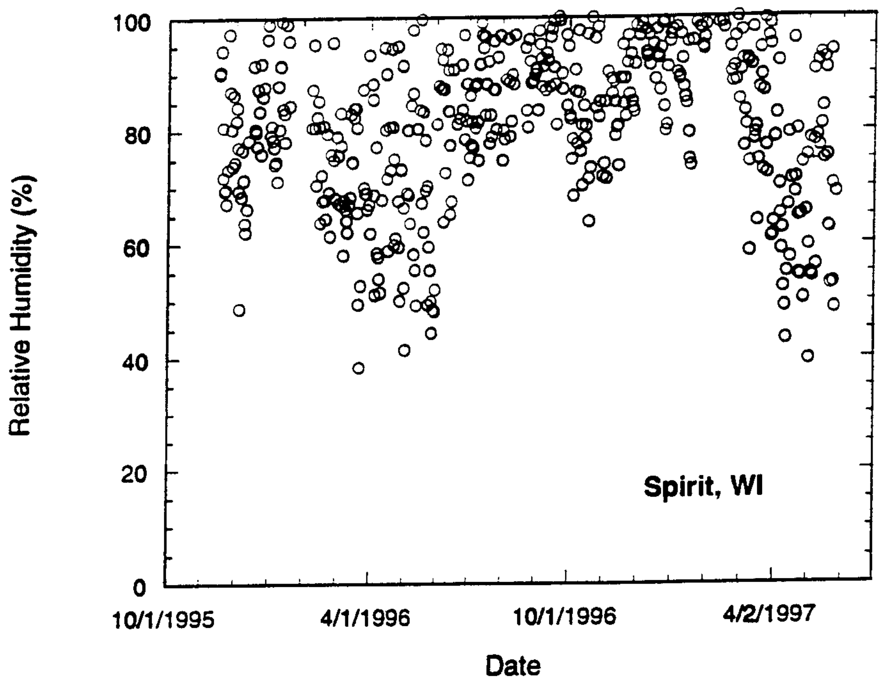
Relative Humidity (%)
100
80
60
40
20
0
Spirit, WI
10/1/1995
4/1/1996
10/1/1996
4/2/1997
Date

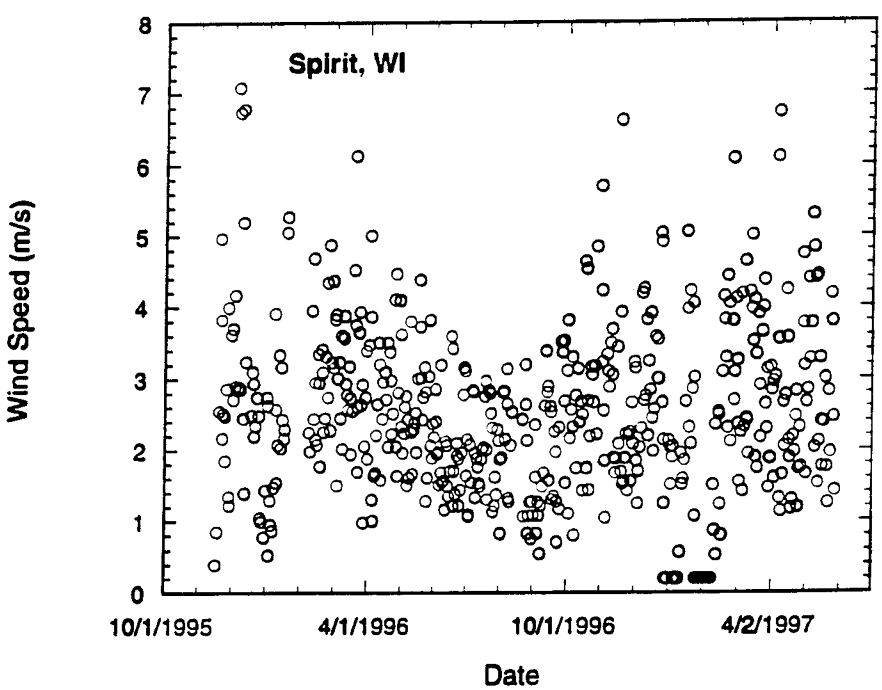
Wind Speed (m/s)
8
7
6
5
4
3
2
1
0
Spirit, WI
10/1/1995
4/1/1996
10/1/1996
4/2/1997
Date

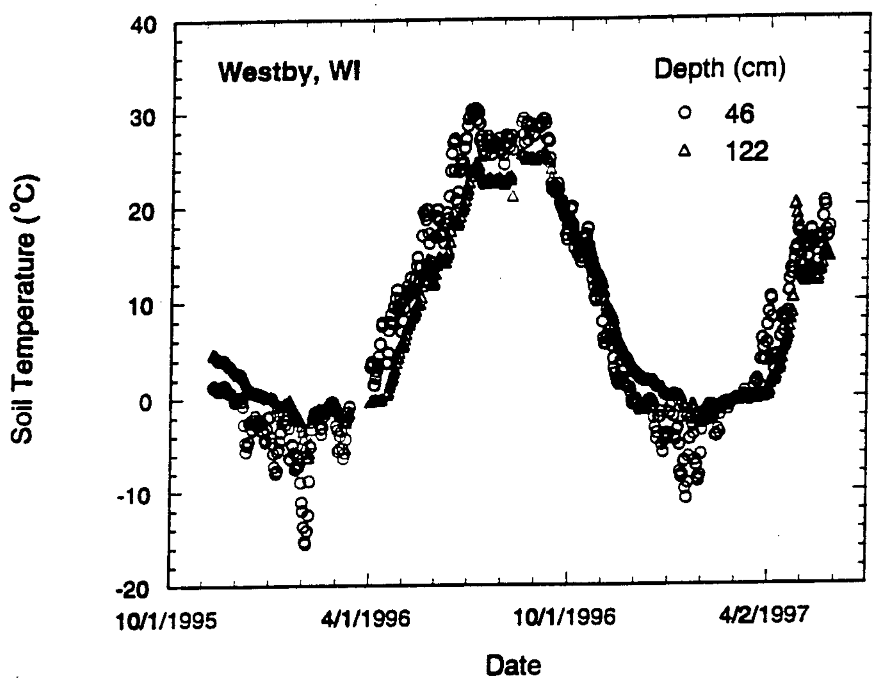
Westby, WI
Depth (cm)
46
122
Soil Temperature (°C)
40
30
20
10
0
-10
-20
10/1/1995
4/1/1996
10/1/1996
4/2/1997
Date

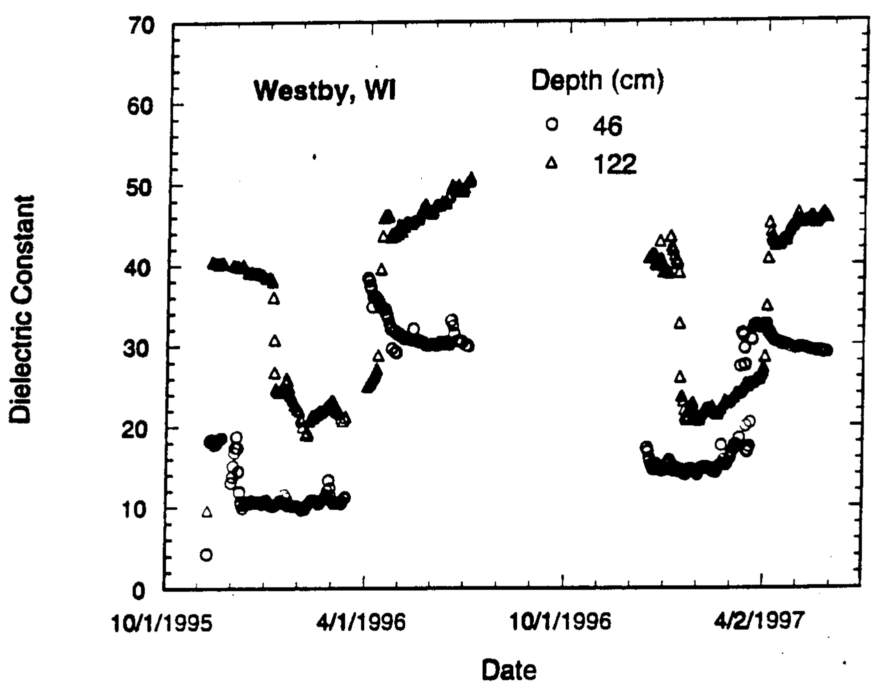
Westby, WI
Depth (cm)
46
122
Dielectric Constant
70
60
50
40
30
20
10
0
10/1/1995
4/1/1996
10/1/1996
4/2/1997
Date

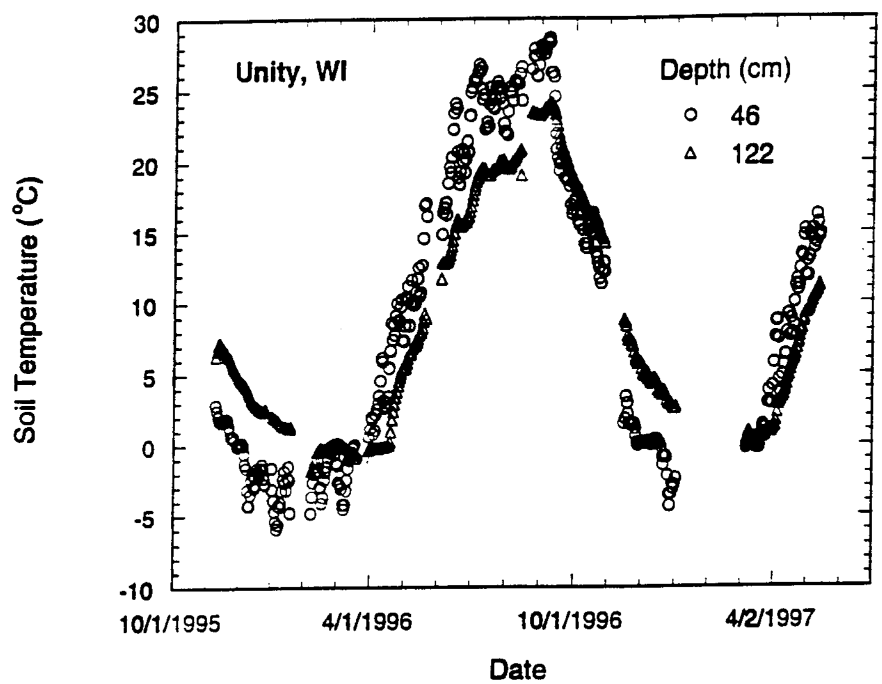
Unity, WI
Depth (cm)
46
122
Soil Temperature (°C)
30
25
20
15
10
5
0
-5
-10
10/1/1995
4/1/1996
10/1/1996
4/2/1997
Date

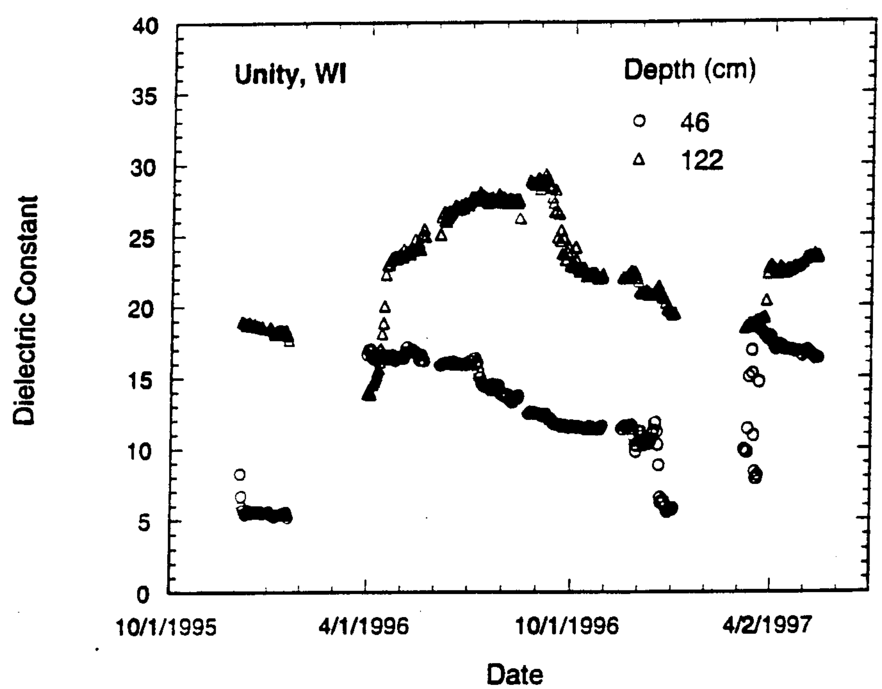
Unity, WI
Depth (cm)
46
122
Dielectric Constant
40
35
30
25
20
15
10
5
0
10/1/1995
4/1/1996
10/1/1996
4/2/1997
Date

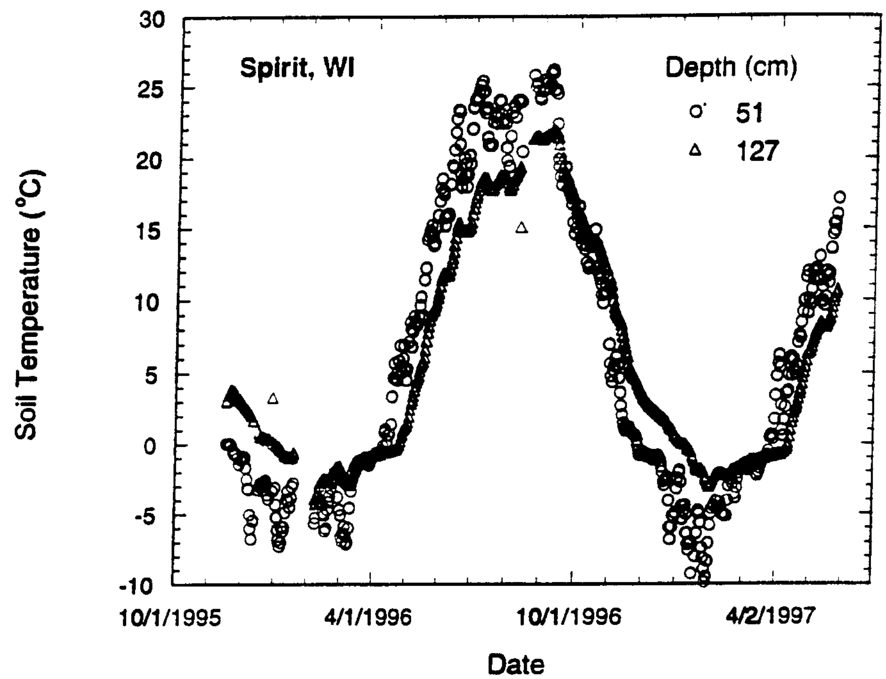
Spirit, WI
Depth (cm)
51
127
Soil Temperature (°C)
30
25
20
15
10
5
0
-5
-10
10/1/1995
4/1/1996
10/1/1996
4/2/1997
Date

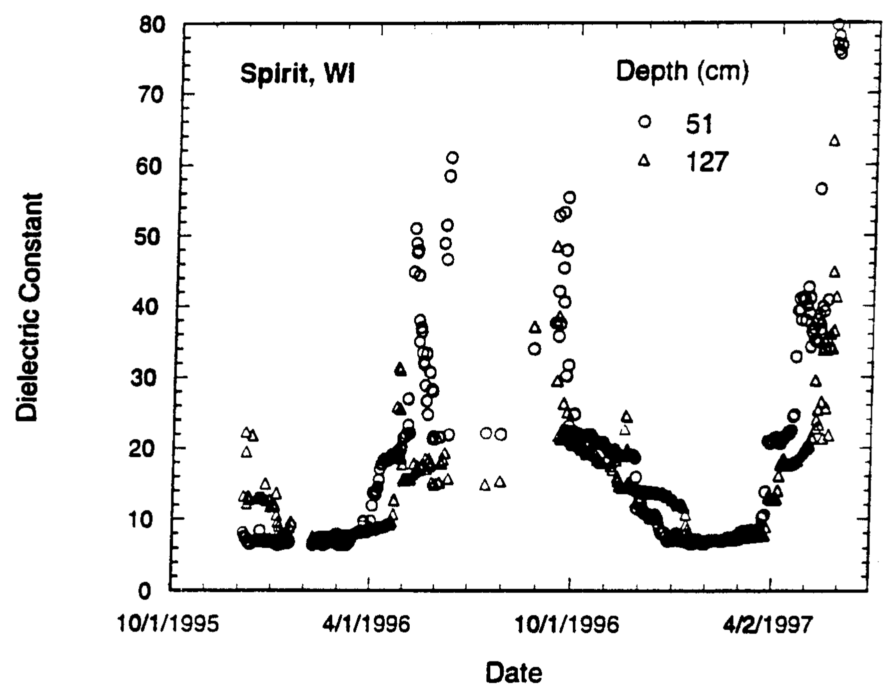
Spirit, WI
Depth (cm)
51
127
Dielectric Constant
80
70
60
50
40
30
20
10
0
10/1/1995
4/1/1996
10/1/1996
4/2/1997
Date